ACS Energy Letters

http://pubs.acs.org/journal/aelccp

FOCUS REVIEW

# Energy Regulation in White-Light-Emitting Diodes

Run Wang, Hengyang Xiang,* Jiawei Chen, Yan Li, Yihui Zhou, Wallace C. H. Choy, Zhiyong Fan, and Haibo Zeng*

Cite This: *ACS Energy Lett.* 2022, 7, 2173−2188

Read Online

ACCESS | Metrics & More | Article Recommendations

**ABSTRACT: Full electroluminescence (EL) white-light-emitting diodes (WLEDs) are currently a focus of research in the development of white light sources, owing to their outstanding potentiality and advantages in energy saving. The achievement of EL white emission always involves balanced co-excitation of multi-color emissive centers (red/green/blue (R/G/B) or blue/orange (B/O)). However, R/G/B/O emitters have different bandgaps, making co-excitation extremely difficult. It is known that excitons formed in a wide-bandgap emitter are easily transferred to any narrow-bandgap emitter. Therefore, the regulation of the energy distribution among multi-color emissive centers is one of the key issues for the realization of white emission and improvement of EL performances and color quality/stability of WLEDs. Currently, many energy regulation strategies have been proposed, promoting the development of full EL-WLEDs. In this Focus Review, we discuss energy-transfer mechanisms and energy regulation strategies in various of WLEDs, including white organic light-emitting diodes (WOLEDs), white quantum-dots light-emitting diodes (WQLEDs), and white perovskite light-emitting diodes (WPeLEDs). Finally, according to their status and challenges, we will offer an outlook, which we hope can inspire researchers and make a contribution to the developments of lighting, display fields, etc.**

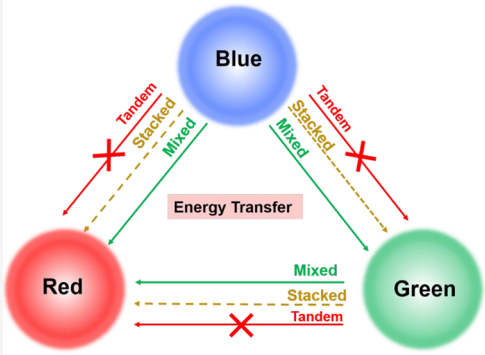


Since the early days of human existence, artificial light sources have been devised with the characteristics of natural sunshine. Such artificial light sources have undergone four generations: oil lamps (flame lighting), incandescent lamps, fluorescent lamps (gas lighting), and light-emitting diodes (LEDs) (semiconductor solid-state lighting, SSL). Flame lighting involves an energy release process from chemical energy to internal energy, during which there is a large amount of energy loss.[1,2] Incandescent bulbs and fluorescent tubes, which convert electricity into internal energy to emit photons, merely convert approximately 5%[2] and 20%[1] of consumed electricity into light, respectively. Therefore, the energy waste rate is still extremely high.[3] In 1996, researchers from Nichia Chemical Co. used a blue InGaN LED chip to excite yellow (Y) phosphors (YAG) and successfully achieved the first white light-emitting diode (WLED),[4] called a phosphors-converting WLED (PC-WLED). PC-WLEDs usually refer to low-energy visible light phosphors excited by high-energy electroluminescence (EL), which typically includes two modes: blue LED chips dominate partial conversion, and UV/near-UV or violet LED chips dominate full conversion. In the partial conversion, part of the blue light emitted from a blue chip by electrical excitation is absorbed by phosphors (Y or Y + red (R)), while the rest is used to combine with phosphors for white light.[5] In the full conversion, the EL light from a UV LED chip is completely absorbed by R + green (G) + blue (B) or white phosphors.[6−11] Compared to the first- and second-generation lighting technologies, the PC-WLEDs show advantages in cutting greenhouse gas emissions and saving energy.[12] Now, PC-WLEDs are the prevailing mainstream lighting technology.[13−15] However, PC-WLEDs are always susceptible to energy loss due to thermal quenching, scattering, and photobleaching.[4] Accordingly, developing WLEDs with high electrical energy utilization is a feasible strategy to reduce the waste ratio of electrical energy. Compared to PC-WLEDs, full EL-WLEDs can directly utilize injected carriers to radiatively recombine for white light. More electrical energy can be used to generate photons, indicating high brightness with low power con-

**Received:** March 14, 2022
**Accepted:** May 18, 2022
**Published:** June 2, 2022

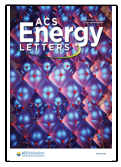

Downloaded via UNIV OF HONG KONG on June 30, 2023 at 04:55:30 (UTC).
See https://pubs.acs.org/sharingguidelines for options on how to legitimately share published articles.

ACS Publications © 2022 American Chemical Society



https://doi.org/10.1021/acsenergylett.2c00610
*ACS Energy Lett.* 2022, 7, 2173−2188

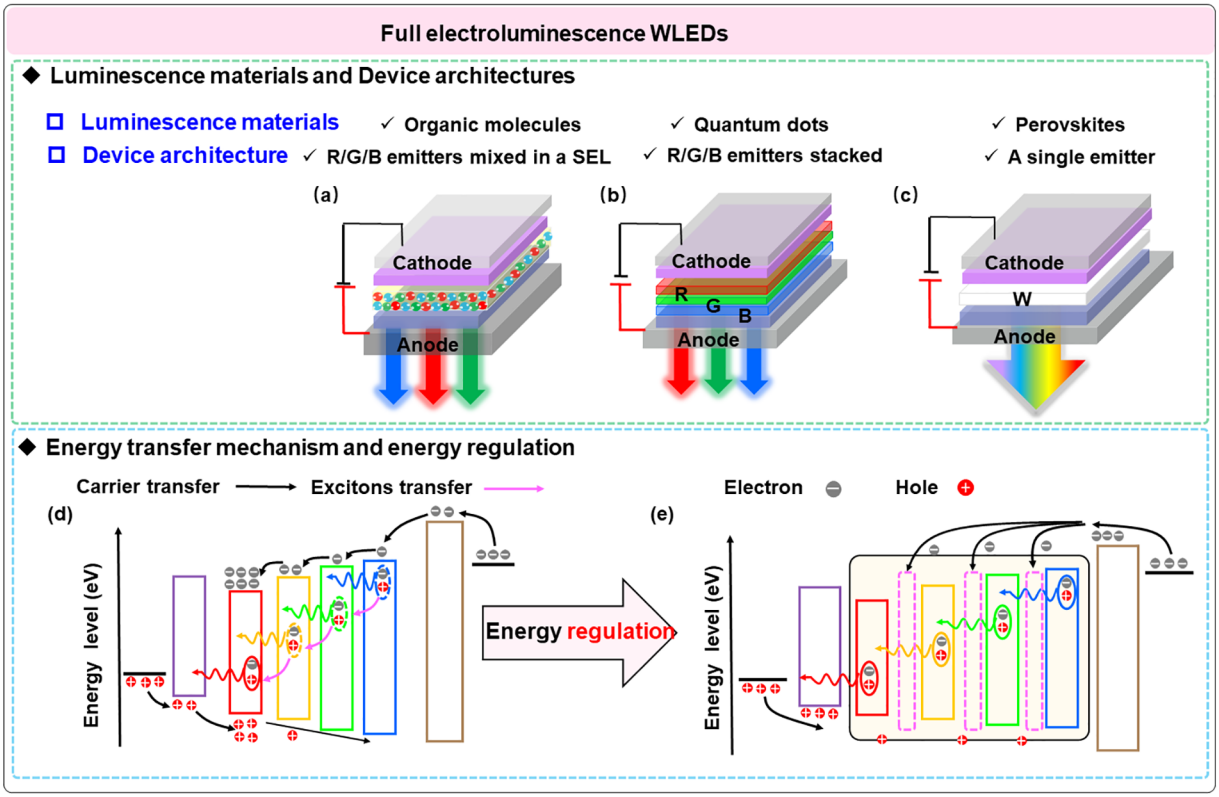


**Figure 1. Luminescence materials, including organic molecules, quantum dots, and perovskites, and device structures of full-WLEDs: (a) multi-color emitters mixed in a SEL; (b) multi-color emitters stacked; and (c) a single emitter. (d) Energy-transfer behavior of different emissive centers in the full EL-WLEDs. (e) After the energy distribution is regulated, multi-color emissive centers generate balanced emissions for white light.**

sumption. Therefore, the development of full EL-WLEDs has presently become a research focus.[4]

According to the statistics, the electricity consumption for lighting accounts for over 15% in total and emits 5% of greenhouse gas all around the world.[16,17] It is predicted that, with the population continuously growing, the demand for lighting will have ascended to 50% of the present consumption by 2030.[18] Thence, the development of new-generation lighting technology, e.g., full EL-WLEDs, is an urgent task.

Full EL-WLEDs are formed by using emitters of complementary colors [blue (B)/orange (O)] or three primary colors [red (R)/green (G)/blue (B)] as emissive layers (EMLs). Currently, highly efficient WLEDs have been developed, which are primarily based on three kinds of luminescent materials: organic molecules, quantum dots (QDs), and perovskites. The color quality and EL performance (efficiency, lifetime) of WLEDs are dominated by many factors: (1) properties of the luminescent materials, such as the optoelectronic properties [e.g., full width at half-maximum (fwhm), photoluminescence yields (PLQYs)] and physical/chemical properties; (2) device structures [e.g., multi-color emitters mixed in a single emitting layer (SEL) (Figure 1a), multi-color emitters stacked (Figure 1b), or a single emitter (Figure 1c)]; and (3) processing technology determined by materials properties and device structures, such as thermal evaporation, spin-coating, and printing. These factors have been widely recognized, analyzed, and summarized[1,17,27−29,19−26] and are guiding the development and application of the WLEDs. However, there is a common key issue affecting the generation of white light, color stability, and device performance of various kinds of WLEDs, which is energy-transfer behavior, but it has received little attention. On one hand, different emissive centers have unequal bandgap values. The wide-bandgap emitter (e.g., B) requires high energy to excite, while the excitation of the narrow-bandgap emitter (R or O) needs relatively low energy. On the other hand, as shown in Figure 1d, excitons formed in the wide-bandgap emitter are easily transferred to any lower ones (e.g., B to G/R or G to R).[26] These energy issues make it difficult for multi-color emissive centers to achieve balanced multi-color emission. This means that energy distribution needs to be controlled effectively for regulating the white light quality and improving the performance of WLEDs (Figure 1e).

> Energy distribution needs to be controlled effectively for regulating the white light quality and improving the performance of white-light-emitting diodes.

Therefore, we considered, it is particularly important to understand the energy-transfer mechanism and behavior and summarize energy regulation strategies in WLEDs, in order to inspire researchers and help make improvements in WLEDs' performance and the development of new WLEDs. In this Focus Review, we dissect the energy-transfer mechanism and summarize its regulation strategies in WOLEDs, WQLEDs and WPeLEDs.


https://doi.org/10.1021/acsenergylett.2c00610
ACS Energy Lett. 2022, 7, 2173−2188

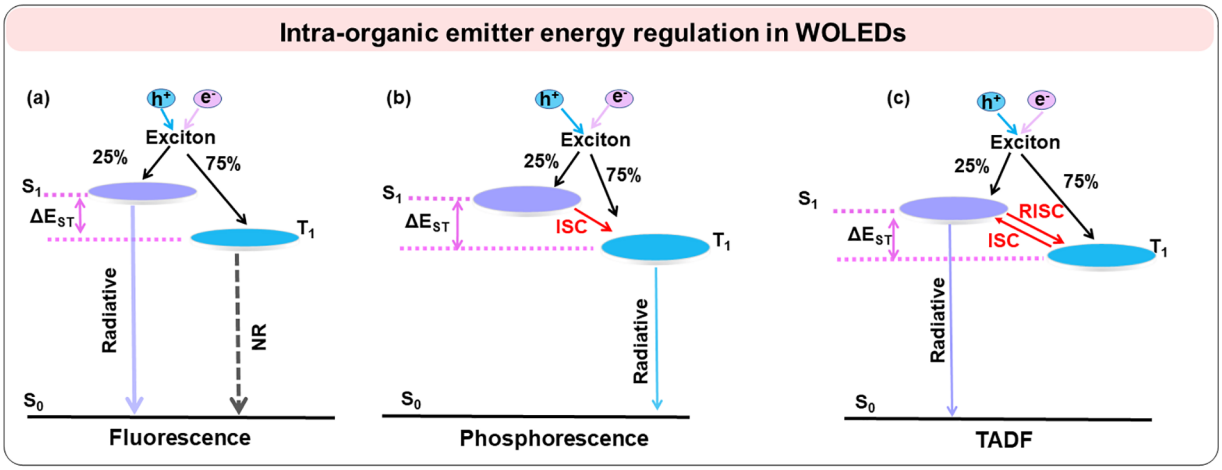


**Figure 2. Schematic diagram of emission mechanism and energy transfer of organic molecules: (a) fluorescent molecule, (b) phosphorescent molecule, and (c) TADF. $S_1$ and $T_1$ are respectively the lowest singlet-state energy level and the lowest triplet-state energy level. $\Delta E_{ST}$ is the difference between $S_1$ and $T_1$. ISC and RISC represent the intersystem and reverse intersystem crossing process, respectively.**

## ■ ENERGY REGULATION IN WOLEDs

In WOLEDs, energy transfer is extremely complex, including not only intramolecular energy transfer but also intermolecular energy transfer. In organic molecules, due to the influence of spin statistics, holes and electrons recombine to form singlet and triplet excitons, accounting for 25% and 75%, respectively. Different organic molecules, i.e., fluorescence, phosphorescence, and thermally activated delayed fluorescence (TADF), have different exciton utilization.[1−3,24] In fluorescence, singlet excitons (25%) can only recombine radiatively, while the remaining triplet excitons decay in the form of non-radiative recombination (Figure 2a), leading to an upper limit of excitons utilization. In phosphorescence, triplet excitons recombine radiatively to emit light. Owing to the heavy-atom effect caused by organic−metal complexes, singlet states ($S_1$) can be harvested by the singlet−triplet intersystem crossing (ISC) process, inducing a maximum excitons utilization of 100%, in theory (Figure 2b). In TADF emitters, the triplet states ($T_1$) can be harvested as delayed fluorescence through the reverse intersystem crossing (RISC) process, which requires a sufficiently small singlet−triplet energy gap difference ($\Delta E_{st}$) in TADF emitters (Figure 2c). Thus, TADF emitters can also achieve 100% exciton utilization in theory. In order to realize high-efficiency WOLEDs, it is first to take advantage of the excitons of these molecules, which is intermolecular energy regulation as mentioned previously. For example, aiming at triplet excitons (75%) of traditional fluorescent molecules, some tactics are exploited to make them useful. In addition to intermolecular energy regulation, intramolecular energy regulation between host−guest or among guests is also particularly significant in the realization of WOLEDs. These energy regulations mainly rely on the different device architectures, for example, multi-color emitters mixed in a SEL and multi-color emitters stacked. Following, energy regulation strategies mixed in SEL- and stacked-WOLEDs will be introduced in detail.

In SEL-WOLEDs, a common strategy to regulate energy is host−guest doping. In one way, a very wide bandgap host is committed to manipulating carrier injection and distribution, while guests can directly capture carriers to form excitons. Another way is that excitons formed in a wide host are transferred to any lower bandgap guests by long-range Förster resonance energy transfer (FRET) for singlet excitons or shorter-range Dexter energy transfer (DET) for triplet excitons. In addition to FRET/DET, excitons in the host can also migrate to the guests by diffusion,[26] where singlet excitons and triplet excitons have different diffusion lengths, respectively about 3 and 100 nm.[30] By these energy regulation methods, different emissive centers can generate balanced emissions, avoiding excessive excitons or carrier distribution in some specific centers (e.g., R or O). In the mixed SEL-WOLEDs, there are primarily three ways in which excitons transfer energy from the host to guests: complete energy transfer (Type 1), partial energy transfer (Type 2), and no energy transfer (Type 3). Notably, among different multi-color emissive centers, there is always a cascade energy transfer from high-energy centers to low-energy ones (B-G-R or B-O).

> In white organic light-emitting diodes, energy transfer is extremely complex, including not only intramolecular energy transfer but also intermolecular energy transfer.

In **Type 1** (complete energy transfer), excitons formed in a wide-bandgap host (n-type, p-type, or bipolar) are completely transferred to guests (R/G/B or B/O) via FRET or DET. In this case, the white light is entirely contributed by guests. As shown in Figure 3a, when R/G/B phosphors serve as guests, singlet excitons/triplet excitons in the host are completely transferred to guests through FRET/DET. R/G/B phosphors can emit balanced tri-color light, which depends on the regulation of dopant concentrations. The complete energy-transfer mechanism is observed in many different types of WOLEDs, e.g., full fluorescent WOLEDs, full phosphorescent WOLEDs, full TADF WOLEDs, and fluorescent/phosphorescent (F/P) hybrid-based WOLEDs.[30−38] In 1994, Kido et al.[39] reported the first fluorescent SEL-WOLED, made by co-doping three fluorescent dyes [DCM 1 (O), coumarin 6 (G), and 1,1,4,4-tetraphenyl-1,3-butadiene (B)] into a host poly(*N*-vinylcarbazole) (PVK). Excitons produced on PVK were transferred to guests, enabling guests to receive energy to be excited for white light. The EL spectrum was tuned by altering B/G/O concentrations, thereby realizing an EL spectrum that can cover


https://doi.org/10.1021/acsenergylett.2c00610
ACS Energy Lett. 2022, 7, 2173−2188

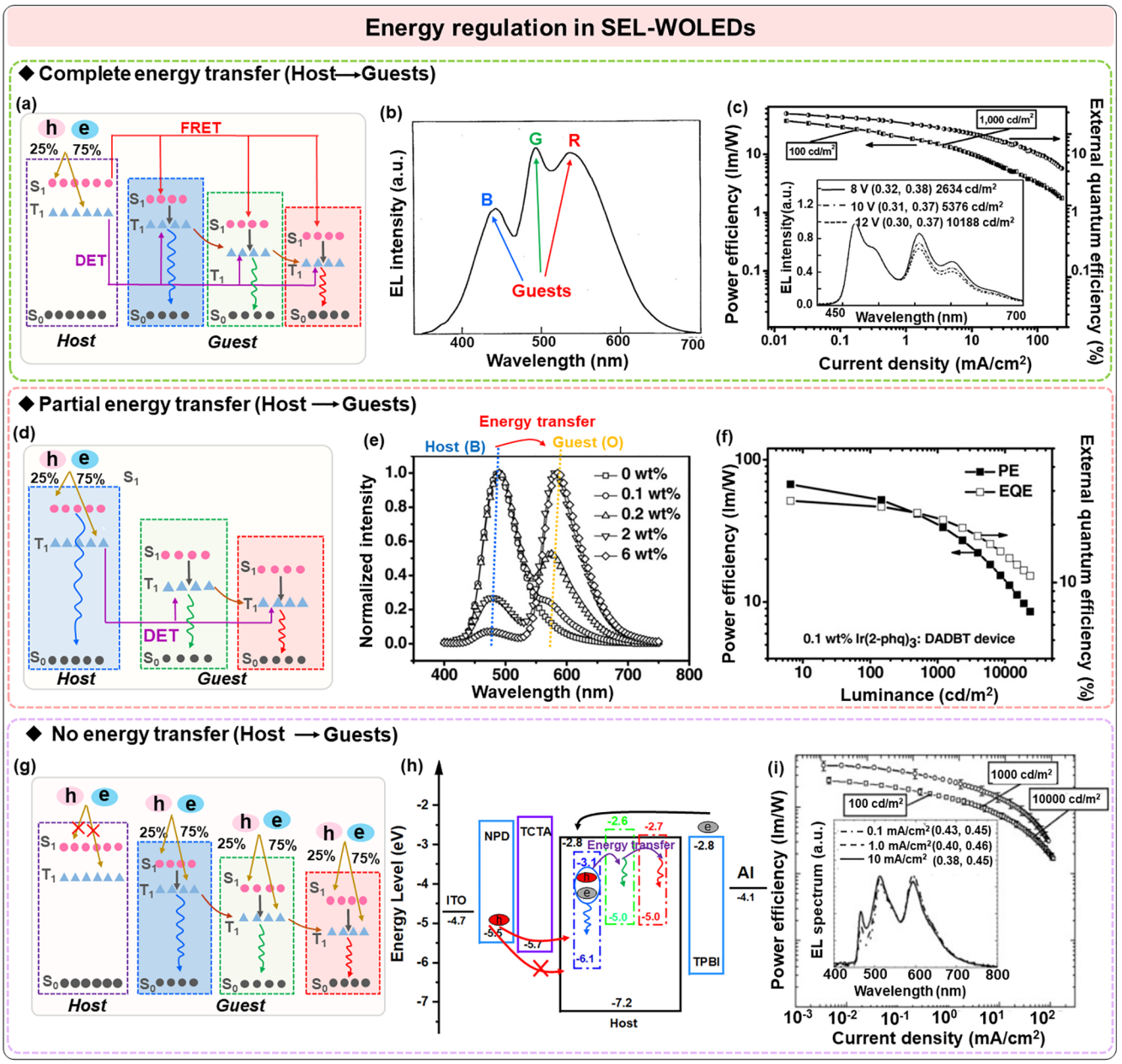


**Figure 3. Energy transfer from the host to guests in SEL-WLEDs. Type 1 (complete energy transfer): (a) Schematic diagram of emission and energy-transfer mechanism. (b) EL spectrum of the first WOLED. Reprinted with permission from ref 39. Copyright 1994 AIP Publishing. (c) Power and EQE as a function of current density for the WOLED. The inset gives the normalized EL spectra and the corresponding CIE coordinates at different brightness. Reprinted with permission from ref 40. Copyright 2009 Wiley-VCH. Type 2 (partial energy transfer): (d) Schematic diagram of emission and energy-transfer mechanism. (e) PL spectrum of DADBT doped with different concentrations of Ir(2-phq)$_3$. (f) PE-L-EQE characteristic of the WOLED (0.1 wt% of Ir(2-phq)$_3$ in DADBT). Reprinted with permission from ref 30. Copyright 2012 Wiley-VCH. Type 3 (no energy transfer): (g) Schematic diagram of emission and energy-transfer mechanism. (h) Energy level diagram of the WOLED and luminescence mechanism. (i) Lighting (circle) and display-relevant (square) power efficiencies versus current and power density. Reprinted with permission from ref 46. Copyright 2004 Wiley-VCH.**

the visible light range (Figure 3b). Owing to the low excitons utilization of fluorescence emitters, WOLED achieved a largest power efficiency (PE) of only 0.83 lm/W. To improve the performance of SEL-WOLEDs, phosphors or TADFs are selected as dopants, owing to their 100% exciton utilization. For instance, Wang et al.[40] used 6.5 wt% phosphor Ir(4,6-dFppy)$_2$(pic) (FIrpic, B) and 0.75 wt% phosphor bis(2-(9,9-diethyl-9*H*-fluoren-2-yl)-1-phenyl-1*H*-benzoimidazol-N,C3)iridium acetylacetonate (fbi)$_2$Ir(acac) (O) co-doped into P-type *N,N′*-dicarbazole-3,5-benzene (mCP) to fabricate a WOLED (Figure 3c). Excitons on mCP were completely transferred to FIrpic by FRET/DET, while (fbi)$_2$Ir(acac) directly employed trapped holes and injected electrons to generate yellow light. Through the two parallel energy channels, B/O emissive centers were co-excited to generate white light. Their WOLED achieved the highest PE and EQE of 42.5 lm/W and 19.3%, respectively (Figure 3c). Additionally, the CIE coordinates of the WOLED were stable, shifting only slightly from (0.33, 0.39) at 1000 cd/


https://doi.org/10.1021/acsenergylett.2c00610
ACS Energy Lett. 2022, 7, 2173−2188

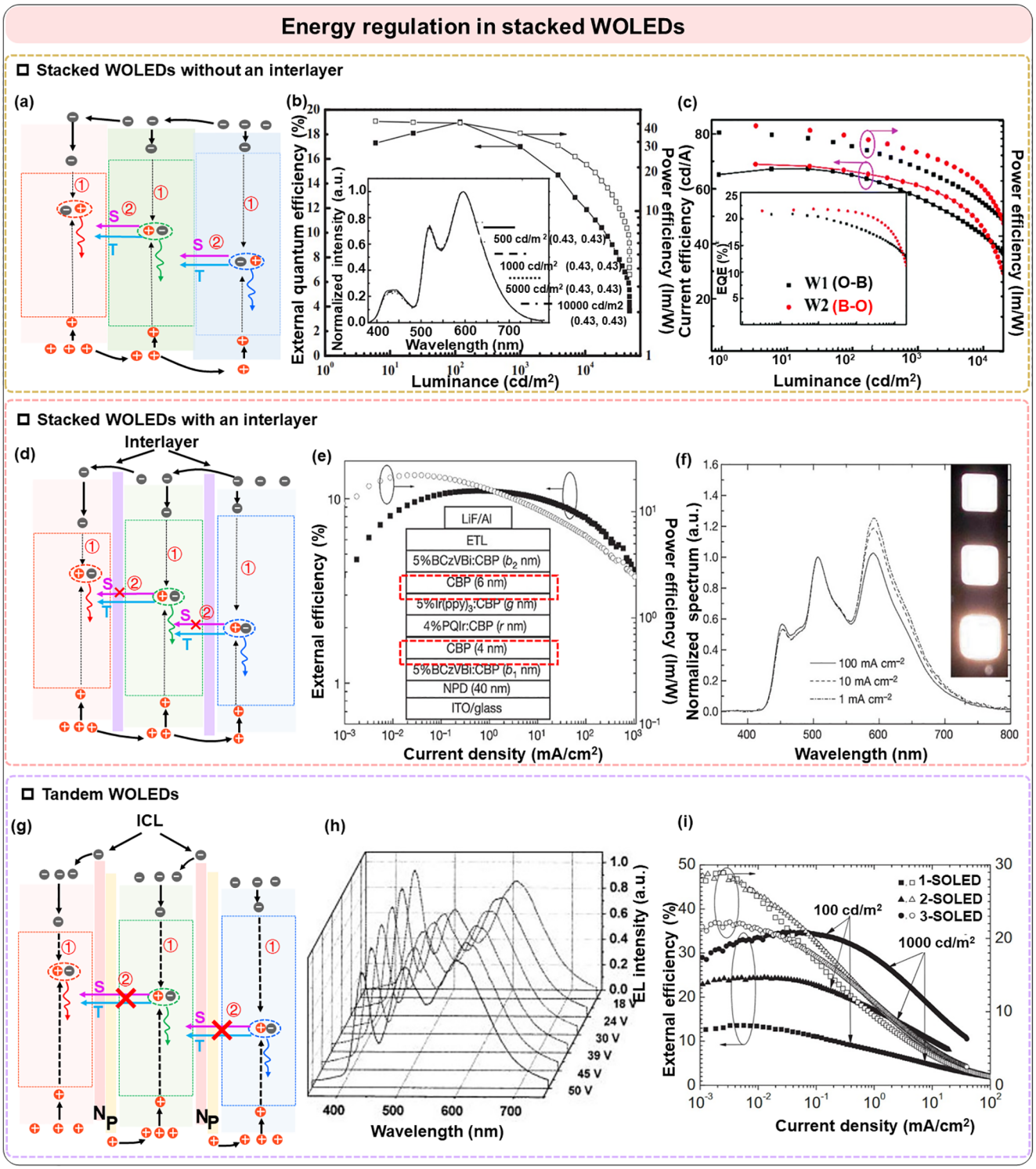


Figure 4. Energy-transfer regulation in stacked WOLEDs. WOLEDs without an interlayer: (a) Schematic diagram of emission and energy-transfer mechanism. (b) EQE and PE versus luminance characteristics of the optimized device. Reprinted with permission from ref 49. Copyright 2013 Wiley-VCH. (c) CE and PE versus luminance characteristics of B-O and O-B stacked WOLEDs. Inset: EQE versus luminance characteristics. Reprinted with permission from ref 52. Copyright 2019 The Royal Society of Chemistry and the Chinese Chemical Society. WOLEDs with an interlayer: (d) Schematic diagram of emission and energy-transfer mechanism. (e) EQE and power efficiency versus the current density of the WOLED are shown in the inset. (f) Normalized EL spectra of WOLED emission at various current densities. Reprinted with permission from ref 62. Copyright 2006 Nature Publishing Group. Tandem WOLEDs: (g) Schematic diagram of emission and energy-transfer mechanism. (h) Normalized EL spectra of the tandem device at different applied voltages. Reprinted with permission from ref 74. Copyright 2005 AIP Publishing. (i) Forward-viewing external and luminous power efficiencies of 1-, 2-, and 3-SOLEDs as functions of *J*. Reprinted with permission from ref 75. Copyright 2006 Wiley-VCH.



https://doi.org/10.1021/acsenergylett.2c00610
ACS Energy Lett. 2022, 7, 2173−2188

$m^2$ to (0.30, 0.37) at a high brightness of 10 000 cd/$m^2$ (see the inset in Figure 3c). Similarly, in 2010, Hou et al.[41] built a SEL-WOLED by co-doping tri-color phosphors [FIrpic (B), tris(2,4-tolylphenylpyridine)iridium ($Ir(mppy)_3$) (G), and bis(1-phenylisoquinoline)(acetylacetonato)iridium(III) ($Ir(piq)_2acac$) (R)] into a mixed host consisting of 9,9-bis[4-(3,6-di-*tert*-butylcarbazol-9-yl)phenyl]fluorene (TBCPF) and 1,3-bis[(4-*tert*-butylphenyl)-1,3,4-oxydiazolyl]phenylene (OXD-7) by a solution process, obtaining a maximum PE of 15.6 lm/W. In their WOLED, the host matrix transferred energy to FIrpic and $Ir(mppy)_3$ for blue/green emission by FRET; meanwhile, part of the green light and all of the red light were created by directly trapping carriers. Of course, sequential cascade energy transfer (B-G-R) also remained. A further approach is to use a TADF as guest because of its exciton utilization of 100% in theory. In 2021, Zhang et al.[42] reported a WOLED with the highest EQE of 20.2%, where the EML was formed by a blue TADF (2,3,4,5,6-pentakis(3,6-dimethyl-9*H*-carbazol-9-yl)benzonitrile, 5PCzCN) and a yellow TADF (1,4-dicyano-2,3,5,6-tetrakis(3,6-diphenylcarbazol-9-yl)benzene, 4CzTPN-Ph) co-incorporated into a mCP host. Singlet/triplet excitons generated on the host were completely transferred to the blue TADF by FRET/DET. Then, the blue TADF emitter transferred energy to the yellow one by a cascade energy transfer. Finally, B/O emissive centers were co-excited to emit white light.

In **Type 2** (partial energy transfer), a blue fluorescent or TADF emitter served as the host. The blue emitter emits blue light and transfers partial energy to guests (R/G or O). Here, white light originated from the co-excitation of the host and guests. As shown in Figure 3d, when the host is a blue fluorescence emitter and guests are R/G/B phosphorescence emitters, singlet excitons on the blue host emit blue light, and triplet states can be transferred to guests by DET. Notably, 75% of triplet excitons in traditional fluorescence can be put to good use, which is beneficial for enhancing excitons utilization. However, if the triplet state of the fluorophore is lower than that of the phosphor, part of the singlet excitons is used to emit blue light, while another part of singlet excitons transfers energy to guests by FRET. In this case, triplet excitons of phosphors can be quenched by the fluorophore, which is not unexpected.[43] Thence, the selection of hosts and guests is particularly critical, as we described above. Besides, in the doping system, if the dopant concentration is very low, it will be difficult to transfer excitons in the host to the dopants, producing only blue fluorescence by the host. In contrast, when the dopant concentration is too high, most of the excitons in the host are transferred to the dopant molecules, meaning blue emission is extremely weak and R/G or O emissions are too strong. Therefore, only when the doping concentration is appropriate, co-emission of the host and guests can be achieved for white light. In 2012, Ye et al.[30] demonstrated a F/P hybrid SEL-WOLED. made by using a doping concentration regulation strategy, where the EML was formed by mixing blue fluorophore 2,8-di[4-(diphenylamino)phenyl]dibenzothiophene-*S*,*S*-dioxide (DADBT) with orange phosphor tris(2-phenylquinoline)-iridium(III) ($Ir(2\text{-}phq)_3$). The researchers explored different doping concentrations ($Ir(2\text{-}phq)_3$: 0, 0.1, 0.2, 2, and 6 wt%). Under the condition of $Ir(2\text{-}phq)_3$ with 0.1 wt%, singlet states can be captured by the host to emit blue light; meanwhile, triplet ones can be transferred to the guest to emit orange light. Therefore, the host and guest achieve co-emission, hence generating a warm white light covering from 425 to 750 nm, as shown in Figure 3e. The WOLED delivered a maximum PE of 67.2 lm/W and EQE of 26.6% (Figure 3f). Besides, if the blue host is TADF, the TADF host emitter will produce blue emissions and simultaneously transfer energy to guests by FRET/DET. Compared to a blue fluorophore as the host, TADF as the host can reduce the waste of triplet excitons. In 2015, Liu et al.[44] co-doped 0.1 wt% $Ir(ppy)_2acac$ and 0.3 wt% $Ir(MDQ)_2acac$ into a blue TADF host (CDBP:$POT_2T$ exciplex) to fabricate an EML, where the blue TADF host transferred energy to G/R phosphors dopants, making R/G/B co-excited. Owing to the high excitons utilization of host TADF, the WOLED achieved a largest EQE of 25.5% and PE of 84.1 lm/W. In 2018, Wang et al.[36] used a blue TADF molecule (TRZ-CF) with bipolar charge-transport properties and a yellow phosphorescent molecule (iridium(III) bis(4-phenylthieno[3,2-*c*]pyridinato-N,C2, PO-01) respectively as the host and the guest to form an EML and constructed a WOLED with the highest EQE of 20.3% and a low-efficiency roll-off.

In **Type 3** (no energy transfer), a wide-bandgap material with carriers transporting capability served as the host−guest emitters (R/G/B or B/O) directly harvesting carriers to recombine and emit light, as shown in Figure 3g. The host plays a role in regulating the carriers distribution rather than transferring energy. Therefore, energy loss caused during the energy transfer from host to guests can be reduced.[1,45] Based on this strategy, in 2004, D'Andrade et al.[46] selected a red phosphor, iridium(III) bis(2-phenylquinolyl-N,C2′)acetylacetonate (PQIr, 2 wt%), and a green phosphor, ($Ir(ppy)_3$, 0.5 wt%), as well as a blue phosphor, bis(4′,6′-difluorophenylpyridinato)tetrakis(1-pyrazolyl)borate ($FIr_6$, 20 wt%), to co-dope into a wide-bandgap *p*-bis(triphenylsilyl)benzene (UGH2) to prepare a SEL-WOLED. Owing to the relatively wide bandgap of UGH2, energy transfer from the host to phosphors was eliminated. In WOLEDs, blue guest $FIr_6$ was excited to emit blue light by trapping the holes and electrons. Then, the blue phosphor transferred energy to the green and red ones, enabling green and red phosphors to be excited for green and red emissions, as shown in Figure 3h. Profiting from the elimination of host−guest energy transfer, energy loss was decreased. As a consequence, the SEL-WOLED showed a maximum EQE of 12.0% and PE of 26.42 lm/W, as shown in Figure 3i. Yet, with the current density increasing, both CIE coordinates and CRI still happened to blue-shift (inset in Figure 3i) as a result of energy transfer between guest emitters.

As we analyzed above, in SEL-WOLEDs emitters with mixed R/G/B or B/O, a careful and precise manipulation of the doping concentrations is required for white emission. However, an especially low doping concentration (generally <1 wt%)[47,48] is extremely difficult to control during the fabrication process. Furthermore, inevitably, multi-color emitters are directly connected, giving rise to excitons quenching. In response to this problem, some device structures were designed and proposed. Typically, multi-color emitters were separated into EMLs and vertically stacked in some order (i.e., R-G-B or B-G-R) to construct stacked WOLEDs. In stacking structures, multi-color emissive centers can have an effective separation, which permits flexible manipulation of every EML and precise control of the excitons' or carriers' distribution in different EMLs.

For stacked WOLEDs, the co-excitation mechanism of multi-color emissive centers includes primarily two processes: as shown in Figure 4a, (1) electrons and holes are injected in hosts and then respectively transferred to guests. The guests capture carriers to radiatively recombine for light. (2) Excitons created


https://doi.org/10.1021/acsenergylett.2c00610
ACS Energy Lett. 2022, 7, 2173−2188

in the high-bandgap emitter are sequentially transferred to low-bandgap emitters, forming cascade energy transfer (e.g., B-G-R or B-O). In 2014, Sun et al.[49] employed a mixed host with bipolar transport ability to fabricate a fluorescent blue EML, 4,4,4-tris(*N*-carbazolyl)triphenylamine (TCTA):1,3,5-tri(*m*-pyrid-3-ylphenyl)benzene (TmPyPB):*N*,*N*′-di-1-naphthalenyl-*N*,*N*′-diphenyl-[1,1′:4′,1″:4′′,1‴-quaterphenyl]-4,4′′′-diamine (4P-NPD). Then, $Ir(MDQ)_2(acac)$ (G) and $Ir(ppy)_2(acac)$ (R) were respectively incorporated into TCTA to form green and red EMLs. The three-primary-color emitters were arranged with a R-G-B sequence from the anode to the cathode to prepare a stacked WOLED. In this WOLED, the main exciton generation region was located at the blue EML. The triplet excitons in TmPyPB were sequentially diffused into the green and red guests by DET, building a cascade energy-transfer channel. Simultaneously, the red and green guests also generated excitons by directly trapping charges for the green and red emissions, owing to their matched energy levels with neighboring functional layers. Benefiting from the bipolar transport properties of the mixed host for blue EML and low-concentration doping of guests, the intrinsically mutual excitons quenching between fluorescent and phosphorescent emitters was effectively restrained. Finally, the WOLED achieved a maximum EQE and PE of 19.0% and 41.7 lm/W, respectively (Figure 4b). Besides, as shown in the inset of Figure 4b, the EL spectrum was rather stable at different luminance, attributed to balancing excitons generation by rationally arranging the stacking structure and the selection and match of hosts and guests. In 2015, Zhu et al.[50] directly chose a bipolar material, 2,6-bis(3-(carbazol-9-yl)phenyl)pyridine (26DCzPPy), as the host of blue phosphor FIrpic (20 wt%) for a blue EML, while red $Ir(MDQ)_2(acac)$ (8 wt%) and green $Ir(ppy)_2(acac)$ (6 wt%) were blended into TCTA to form red and green EMLs, respectively. Then, a stacked WOLED in a sequence of R-G-B was prepared, which manifested the highest PE of 46.6 lm/W and EQE of 22.4%. In 2016, a TADF-based hybrid stacked WOLED was demonstrated by their team.[51] They employed a blue TADF emitter with bipolar charge-transporting capability to dope with ((diphenylphosphino)phenyl)ether oxide (DPEPO) for blue EML, and then 8 wt% red $Ir(PPQ)_2acac$ and 8 wt% green $Ir(ppy)_2acac$ were doped into TCTA for red and green EMLs, respectively. By utilizing the B-G-R cascade energy transfer and precisely manipulating carriers and excitons distribution, the resulting WOLED exhibited a maximum EQE, CE, and PE of 23%, 51.0 cd/A, and 51.7 lm/W, respectively. The CIE coordinates were located at (0.438, 0.438), and CRI was 89. In 2019, Ying et al.[52] discussed the influence of the arrangement sequence of EMLs on the WOLEDs. Figure 4c shows the CE and PE versus luminance characteristics of the two WOLEDs, respectively corresponding to stacking EMLs with B-O and O-B sequences. The WOLED with B-O order obtained a higher EL performance, compared to that with O-B order. A similar phenomenon also was observed in a three-color stacked WOLED. These results indicated that the rational arrangement sequence of EMLs is conducive to improving energy utilization in devices, thereby boosting the performance of WOLEDs.

As we discussed previously, in both SEL-WOLEDs and stacked WOLEDs, excitons in a large-bandgap EML (e.g., blue) are always transferred to any smaller bandgap EMLs by a cascade energy-transfer (B-G-R or B-O) channel. However, the energy-transfer process easily induces energy loss[53] and results in an unstable EL spectrum in WOLEDs with the increasing operating voltages.[54] An effective approach to improve this involves inserting a thin interlayer with carrier transport capability (i.e., bipolar or unipolar materials)[55−62] between different EMLs, so that the stacked EMLs are separated in space, as shown in Figure 4d. The spacer layer contributes to blocking part of the excitons migration (i.e., the singlet excitons with short diffusion lengths) and suppressing some unwanted energy-transfer processes. In 2006, Sun et al.[62] placed a bipolar interlayer 4,4′-*N*,*N*′-dicarbazolylbiphenyl (CBP) between blue and red/green EMLs to fabricate a stacked WOLED, as shown in the inset of Figure 4e. Thanks to the introduction of the CBP spacer layer, singlet excitons formed in the host were transferred to the adjacent blue fluorescent emitter (BCzVbi) by FERT, but not to phosphorescent dopants, since singlet excitons had a short diffusion length. Accordingly, the insertion of CBP prevented direct energy transfer from the blue dopant to the green and red phosphors, minimizing energy loss. Nevertheless, triplet excitons in the blue fluorescent emitter can effectively migrate into green and red phosphorescent emitters by a long diffusion length process (about 100 nm), effectively avoiding triplet excitons' non-radiative recombination.[30] Therefore, in this unique structure, singlet and triplet excitons were completely captured by independent channels, enhancing excitons utilization. As a result, the WOLED achieved a peak EQE of 18.7% and PE of 37.6 lm/W, as shown in Figure 4e. Figure 4f exhibits the EL spectrum of the WOLED at different current densities and corresponding real images of devices. Owing to the required high energy for excitation of blue phosphor, blue emission became stronger with increasing applied voltage. Hence, the CIE coordinates also exhibited an apparent shift. In 2014, the same researchers used a similar strategy to fabricate a tri-color (R/G/B) stacked WOLED with the largest PE of 40.7 lm/W and EQE of 21.2%.[63] In this work, the CBP interlayer was inserted between the green (CBP: 3 wt% $Ir(ppy)_3$) and red (CBP: 6 wt% $Ir(MDQ)_2(acac)$) regions, decreasing exciton quenching caused by energy transfer from $Ir(ppy)_3$ ($T_1$ = 2.4 eV) to $Ir(MDQ)_2(acac)$ ($T_1$ = 2.0 eV). In 2019, Chen et al.[64] selected mCP as an interlayer that was sandwiched between a sky-blue TADF emitter and a red fluorescence emitter. Owing to its high $T_1$ (2.9 eV), mCP effectively suppressed the DET of triplet excitons from blue TADF to red fluorescence, preventing triplet excitons from quenching. Consequently, the WOLED with an interlayer of mCP exhibited a higher EQE of 23% compared to that without any interlayer (EQE = 11%).

The introduction of kinds of interlayers above can block part of excitons diffusion and suppress some energy-transfer processes, serving to improve the color stability of WOLEDs, but such structures may cause a decrease in device efficiency.[65,66] Accordingly, it is difficult to get a trade-off between device efficiency and color stability.

In order to ensure that efficiency is not affected or is even improved while regulating energy-transfer behavior and blocking excitons diffusion, instead of separating the different emitters into different EMLs, interconnecting layers (ICLs), composed of N- and P-type semiconductors, can be used to connect different complete EL units for WOLEDs, called tandem WOLEDs. As shown in Figure 4g, The EL units can be not only complementary colors (B-O) or three primary colors (R-G-B) but also a white light unit for WOLEDs. The goal of adopting the tandem concept is to improve the efficiency, operational stability, and color stability of WOLEDs. Instead of achieving at most one photon per unit carrier, thanks to ICLs with excellent carrier generation ability, tandem devices can generate multiple photons per unit charge.[67,68] In tandem WOLEDs, it is


https://doi.org/10.1021/acsenergylett.2c00610
ACS Energy Lett. 2022, 7, 2173−2188

significant to design and optimize ICLs. Benefiting from the exploitation and optimization of different ICLs, some tandem WOLEDs with high efficiency and color stability have been successfully achieved.[69−73] The first tandem WOLED was based on R/G/B fluorescent emitters, where ICL was BCP:Li/$V_2O_5$.[74] With the voltage increasing, the tandem WOLED showed a stable white light (Figure 4h), with CIE coordinates from (0.35, 0.32) at 18 V to (0.36, 0.36) at 50 V. The obtained maximum brightness and efficiency were basically equal to the sum of the EL units, ascribed to the strong carrier generation role of the ICL. In 2006, Kanno et al.[75] used an ICL (Bphen:Li/$MoO_3$) to fabricate tandem WOLEDs based on a white EL unit, with two or three EL units (corresponding to a 2-SOLED or 3-SOLED). As shown in Figure 4i, as the number of white EL units increases, the efficiencies of the corresponding WOLED also increase.

## ■ ENERGY REGULATION IN WQLEDs

WQLEDs are realized by co-exciting R/G/B and B/O QDs. Different from WOLEDs, QDs have no complex intramolecular energy-transfer behavior and host−guest doping system. Therefore, in WQLEDs, the energy regulation strategies mainly aim at energy-transfer behavior among multi-color QDs' emission centers. It mainly includes controlling QDs' mixing ratios for SEL-WQLEDs and optimizing device structures for stacked WQLEDs, e.g., similar to WOLEDs, the introduction of an interlayer or ICLs between stacking EMLs.

> In white quantum-dots light-emitting diodes, the energy regulation strategies mainly aim at energy-transfer behavior among multi-color quantum dots' emission centers.

In R/G/B mixed SEL-WQLEDs, without a host−guest matrix, R/G/B and B/O QDs are mutually contacted, as shown in Figure 5a. R/G/B QDs emit light by capturing electrons and holes. Excitons formed in a wide-bandgap emissive center can transfer to any low-bandgap emissive centers by FRET, i.e., B to G, B to R, and G to R. This will lead to excitons' energy loss and serious excitons quenching, so R/G/B mixed SEL-WQLEDs always exhibit poor efficiency and an unstable emission spectrum. To tune the emission ratio of different emissive centers and regulate energy transfer among different QDs, it is necessarry to strictly manipulate the R/G/B mixing ratios. Generally, the doping ratio of blue QDs is the largest, ensuring that the blue QDs retain sufficient blue light after the energy transfer to G/R QDs. In 2007, Bulović et al.[76] demonstrated the first R/G/B QDs mixed WQLED (R:G:B = 1:2:10), with the highest EQE of only 0.36% and CIE coordinates located at (0.35, 0.41). With the development of QDs synthesis technologies, QDs with high PLQY and matched carrier injection interfaces were fabricated, facilitating the improvement of WQLEDs. In 2015, Lee et al.[77] blended R (ZnS/CdSeS)/G (ZnS/CdZnSeS)/B (ZnS/CdZnS) QDs to form an EML for a WQLED. By optimizing mixing ratios, the realized WQLED showed the largest EQE of 10.9% and CE of 21.8 cd/A. However, this WQLED showed unstable emission, especially a low driving voltage range. As shown in Figure 5b, at a low bias of 4 V, only a red EL was observed (inset in Figure 5b), attributed to red QD with the smallest band gap among R/G/B ones. Upon increasing driving voltage, the EL intensity of green and red QDs exhibited respectively a slight and sharp reduction, as shown in Figure 5c. Consequently, the CIE color coordinates shifted progressively from (0.453, 0.333) at 5 V to (0.222, 0.293) at 9 V (inset of Figure 5c), which was primarily attributed to the electric-field-assisted inter-QD charge migration and unavoidable excitons energy transfer. The same problem also appeared in other R/G/B mixed SEL-WQLEDs.[78]

Mixed SEL-WQLED devices, owing to inevitable charge/exciton energy transfer among R/G/B QDs, suffered from unstable emission color and low EQE. Even if R/G/B QD EMLs are stacked, R/G/B QDs still can contact each other at the interfaces. Therefore, the energy transfer and excitons quenching still occur.[79] For these issues, like for WOLEDs, a single interlayer (buffer) with carrier transport capacity or even ICLs with strong carrier generation capability are also introduced into WQLEDs.

In WQLEDs with an interlayer, the interlayer can separate the stacked QD EMLs in space, as shown in Figure 5d, so it helps alleviate the excitons energy transfer and block charge/excitons migration, e.g., blocking excitons migration from blue QDs to red QDs. Besides, the single interlayer also helps to balance the carrier transport in WQLEDs. In 2018, Lee et al.[80] reported a R/G/B stacked WQLED, formed by adopting an ultrathin layer of ZnO NPs as an interlayer. The WQLED got the maximum CE of 15.9 cd/A and EQE of 6.8%. However, at low driving voltages (@≤6 V), major emissions stemmed from the red and green QDs, and blue emission was extremely weak, which was due to the diffusion of excitons from B to G and subsequent G to R through FRET, as exhibited in Figure 5e. In high-voltage regions (@≥7 V), sufficient holes were injected in blue QDs, and holes in blue QDs can be transferred to adjacent green and further to red QDs. Thence, excitons were formed in entire QD EMLs, which yielded three primary color emissions and relatively stable CIE coordinates (@≥7 V), as displayed in Figure 5f. Wang et al.[81] proposed to introduce $Zn_{0.95}Mg_{0.05}O$ nanocrystals (NCs) to serve as an interlayer in the WQLEDs, because of their lower defect density and higher conduction band minimum (CBM) compared to ZnO nanoparticles (NPs). Thus, excitons quenching was reduced, and the optimal WQLED gave the highest CE of 24.6 cd/A and PE of 25.8 lm/W. Besides inorganic materials, organic molecule films can also be utilized as an interlayer. For instance, Zhang et al.[82] adopted an organic pre-TBD as an interlayer to gain a WQLED with the biggest EQE of 9.6%. As we mentioned, an interlayer only relieved part of the energy-transfer behavior, rather than completely suppressing FRET and blocking charge migration among R/G/B QDs, so these WQLEDs with an interlayer still showed unstable emission.

To completely suppress energy transfer and charge migration between different bandgap QDs layers, ICLs are incorporated between QDs EMLs, as shown in Figure 5g. In the work reported by Zhang et al. in 2018,[83] the authors simultaneously built three groups of WQLEDs: (1) a mixed SEL-WQLED with a structure of ITO/PEDOT:PSS/PVK/(RGB) mixing QDs/ZnMgO/Al; (2) two double-unit tandem WQLEDs, where TW1[O (G:R)-B] was ITO/PEDOT:PSS/PVK/(G/R)-mixed QDs/ICL/PVK/B-QDs/ZnMgO/Al and TW2 [B-O(G:R)] was ITO/PEDOT:PSS/PVK/B-QDs/ICL/PVK/(G/R)-mixed QDs/ZnMgO/Al; (3) a three-unit tandem WQLED with ITO/PEDOT:PSS/PVK/B-QDs/ICL/PVK/G-QDs/ICL/PVK/R-QDs/ZnMgO/Al. ICLs of all tandem WQLEDs were ZnMgO/Al/HAT-CN/$MoO_3$, as shown in Figure 5h. The results showed that the EQE of the tandem WQLED with three EL units (R-G-


https://doi.org/10.1021/acsenergylett.2c00610
ACS Energy Lett. 2022, 7, 2173−2188

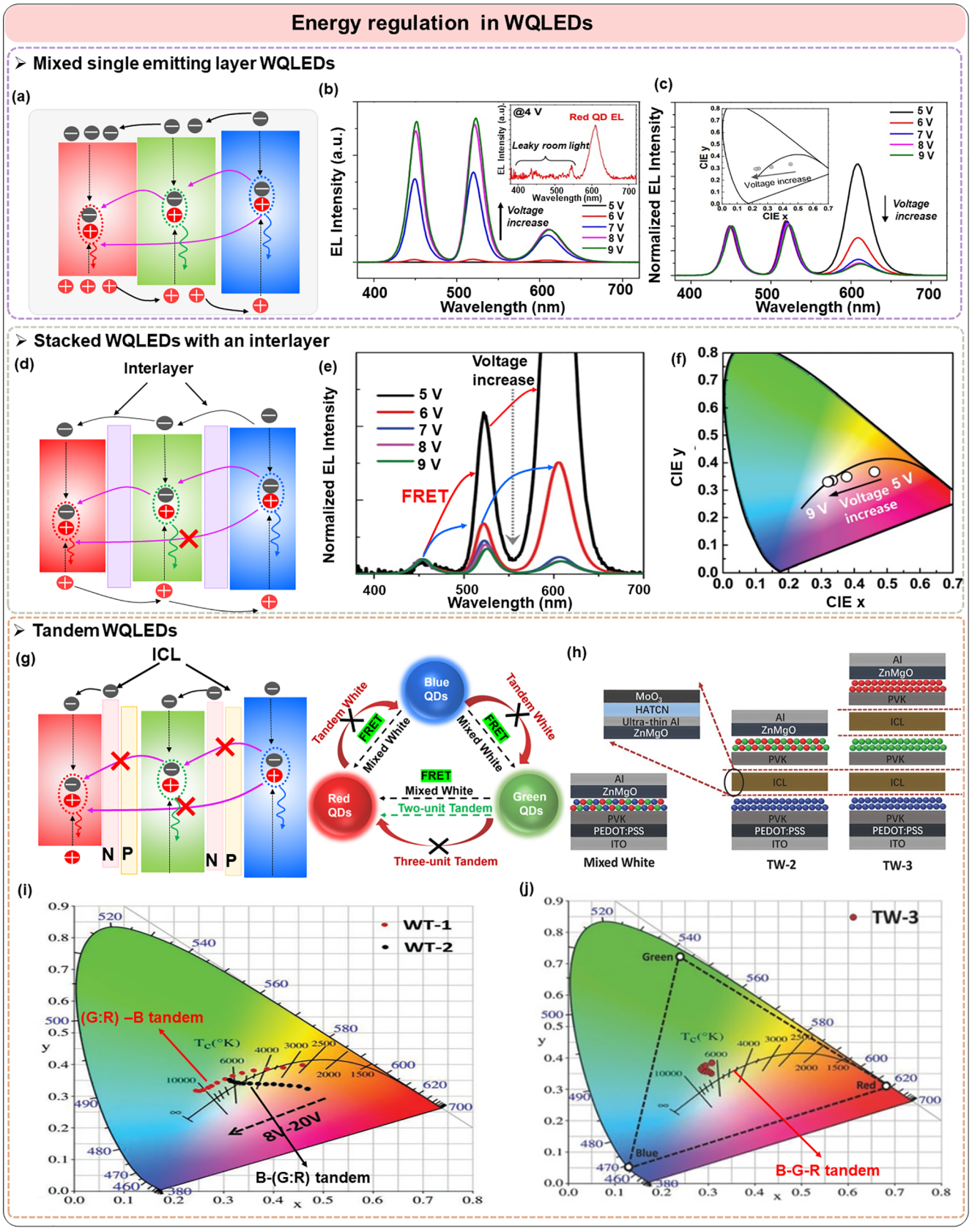


Figure 5. Energy-transfer regulation in WQLEDs. Mixed SEL-WQLEDs: (a) Schematic diagram of emission and energy-transfer mechanism, (b) voltage dependence as recorded, and (c) normalized EL spectral evolutions of WQLEDs with the variation of CIE color coordinates (inset).[77] Stacked WQLED with an interlayer: (d) Schematic diagram of emission and energy-transfer mechanism, (e) EL spectra of WQLEDs and (f) CIE color coordinates at different voltages. Reprinted with permission from ref 80. Copyright 2018 The Royal Society of Chemistry. Tandem WQLEDs: (g) Schematic diagram of emission and energy-transfer mechanism, (h) schematic device structure of mixed single


https://doi.org/10.1021/acsenergylett.2c00610
ACS Energy Lett. 2022, 7, 2173−2188

**Figure** 5. continued

**WQLEDs, two-unit tandem WQLEDs, and three-unit tandem WQLEDs, (i) CIE coordinates of two-unit WQLEDs at different driving voltages, and (j) CIE coordinates of R-, G-, and B-QLEDs and three-unit WQLEDs. Reprinted with permission from ref 83. Copyright 2018 Wiley-VCH.**

B) was higher than that of the tandem WQLED with two EL units (B-O), and both were higher than that of SEL-mixed WQLEDs. In terms of color stability, as shown in Figure 5i, for both tandem WQLEDs with two EL units, the CIE coordinates exhibited a marked shift with driving voltage varying. Yet, CIE coordinates of one with three EL units displayed extreme stability (Figure 5j). The discrepancies in efficiency and color stability are mainly due to excitons energy transfer and charge migration in the mixed-color EMLs. Following the route of introducing ICLs, in 2018, Jiang et al.[84] designed ZnO/PMA as the ICL to achieve a WQLED with the biggest EQE of 27.3%. Cao et al.[85] adopted PVK/PEDOT:PSS/ZnO/PEIE as an ICL to fabricate a WQLED with a higher EQE of 28%.

## ■ ENERGY REGULATION IN WPeLEDs

WOLEDs and WQLEDs have experienced decades of development and accumulated many effective energy regulation strategies, which facilitated progress in the development of white light sources and exerted a huge effect on exploiting other emerging luminescent materials and WLEDs, i.e., WPeLEDs. With the aid of energy regulation approaches as we mentioned above, WPeLEDs have made significant research progress in recent years. On one hand, following the technology route of WOLEDs and WQLEDs, mixed SEL-WPeLEDs and stacked-WPeLEDs have been successfully achieved. On the other hand, some single-emitter WPeLEDs with broad-spectrum white light have been developed, derived from self-trapped excitons (STEs) based on perovskites or elements doped ones.

> Some single-emitter white perovskite light-emitting diodes with broad-spectrum white light have been developed, derived from self-trapped excitons based on perovskites or element-doped perovskites.

In R/G/B mixed SEL-WPeLEDs, Yu et al.[86] mixed halide perovskites (CsI, $PbBr_2$, and BHCl) to form a perovskite EML film by spin-coating. By optimizing the doping ratios of each component for regulation of energy distribution, a pure white PeLED acquired a peak EQE of 0.008%. In a stacked structure, Mao et al.[87] adopted BIPO/Poly-TPD as an ICL to suppress energy transfer between $PA_2CsPb_2I_7$ and $CsPb(Br_xCl)_3$. The fabricated tandem WPeLED successfully emitted white light with a CIE of (0.32, 0.32) and achieved a peak radiance of 0.17 W/(Sr·m$^2$). These WPeLEDs exhibited low performance, largely caused by the poor photoelectric properties of perovskites and incompatible solvent during solution processing. Besides, hybrid halide perovskites are prone to ion migration under electric field driving, resulting in the poor EL performance of R/G/B mixed SEL-/stacked-WPeLEDs. Hence, for improving mixed SEL-WPeLEDs or stacked-WPeLEDs, perovskites were often mixed with organic molecules to form hybrid WLEDs,[17] where energy-transfer regulation was similar to that previously mentioned. For example, Liu et al.[88] reported a perovskite/organic hybrid WLED with a peak EQE of 7.35%. An ultrathin phosphorescent interlayer was inserted between a p-type hole transport layer and an n-type electron transport layer, forming an organic p-i-n heterojunction unit. Profiting from the insertion of p-HTL, energy transfer between the perovskite layer and the organic phosphorescent interlayer was perfectly suppressed, thus generating white light.

In broad-spectrum WPeLEDs based on STEs, due to the soft lattice properties of perovskites, electrons and holes easily cause lattice distortion and can be trapped by the lattice, promoting the formation of STEs. As shown in Figure 6a, free excitons can transfer energy to STEs, enabling STEs to be excited and emit broad luminescence.[89] Currently, among perovskites with STEs properties, broad-spectrum WPeLEDs were achieved successfully, primarily based on double perovskites ($Cs_2AgInCl_6$[90] and $Cs_2AgIn_{0.9}Bi_{0.1}Cl_6$[91]), copper-based perovskites ($CsCu_2I_3$/$Cs_3Cu_2I_5$[12,92]), and all-inorganic perovskites ($CsPbI_3$[93]). However, the poor carrier transport ability of STE materials limited the efficiency of STE-based WPeLEDs,[12,90−92] but their CRIs were above 90. For improving carrier transport performance, Chen et al.[94] introduced an organic additive, polyethylene glycol sorbian monooleate (Tween), into the perovskite solution of $CsCu_2I_3$ and $Cs_3Cu_2I_5$ and then built a WPeLED with a structure of ITO/PEDOT:PSS/perovskites/TmPyPB/LiF/Al (Figure 6b). Since the additive facilitated the holes injection and transport, this WPeLED exhibited an improved EQE of 3.1% (Figure 6c). $CsPbI_3$ is a heterophase halide perovskite that easily suffers from phase transition from $\alpha$-$CsPbI_3$ to $\delta$-$CsPbI_3$, where $\delta$-$CsPbI_3$ has a broadband feature of STEs. Chen et al.[93] adopted $CsPbI_3$ as an EML to fabricate a PeLED and managed phase transition by controlling the annealing treatment time, making $\alpha/\delta$-$CsPbI_3$ evenly distributed in the EML. As shown in Figure 6d, in the $\alpha/\delta$-$CsPbI_3$ EML, owing to the strong carrier transport capability of $\alpha$-$CsPbI_3$, lots of electrons and holes were injected in $\alpha$-$CsPbI_3$ to form excitons for red emission. Meanwhile, owing to the matched energy level between $\alpha$-$CsPbI_3$ and $\delta$-$CsPbI_3$, carriers and excitons can also transfer to $\delta$-$CsPbI_3$ in a strong electric field, causing excitons to be formed in $\delta$-$CsPbI_3$ for broadband emission. As a result, the PeLED emitted a white light covering the visible light region (Figure 6e). In this work, the poor carrier transport performance of $\delta$-$CsPbI_3$ STE was overcome by the efficient energy transfer of dual phases, thereby boosting the performance of the WPeLED. The WPeLED achieved the largest EQE of 6.5% and the highest luminance of 12 200 cd/m$^2$ (Figure 6f).

Host−guest energy transfer is also applied in perovskites. Some special ions as guests, i.e., $Mn^{2+}$,[95,96] and rare earth (RE) ions,[97] are doped into the perovskite host, which can form multiple emissive centers owing to the newly formed low energy levels, as shown in Figure 6g. Excitons produced on the perovskite host can emit the perovskite's intrinsic emission; meanwhile, energy can be transferred to new emissive centers. Eventually, different emissive centers (B/G/R/O) are co-excited to generate white light. Inspired by the energy-transfer mechanism, Sun et al.[97] used earth ions ($Sm^{3+}$) to dope into $CsPbCl_3$ NCs and formed new energy levels (R/O) belonging to $Sm^{3+}$. Under the electric field, through energy transfer from host materials $CsPbCl_3$ to $Sm^{3+}$ and directly harvesting injected


https://doi.org/10.1021/acsenergylett.2c00610
ACS Energy Lett. 2022, 7, 2173−2188

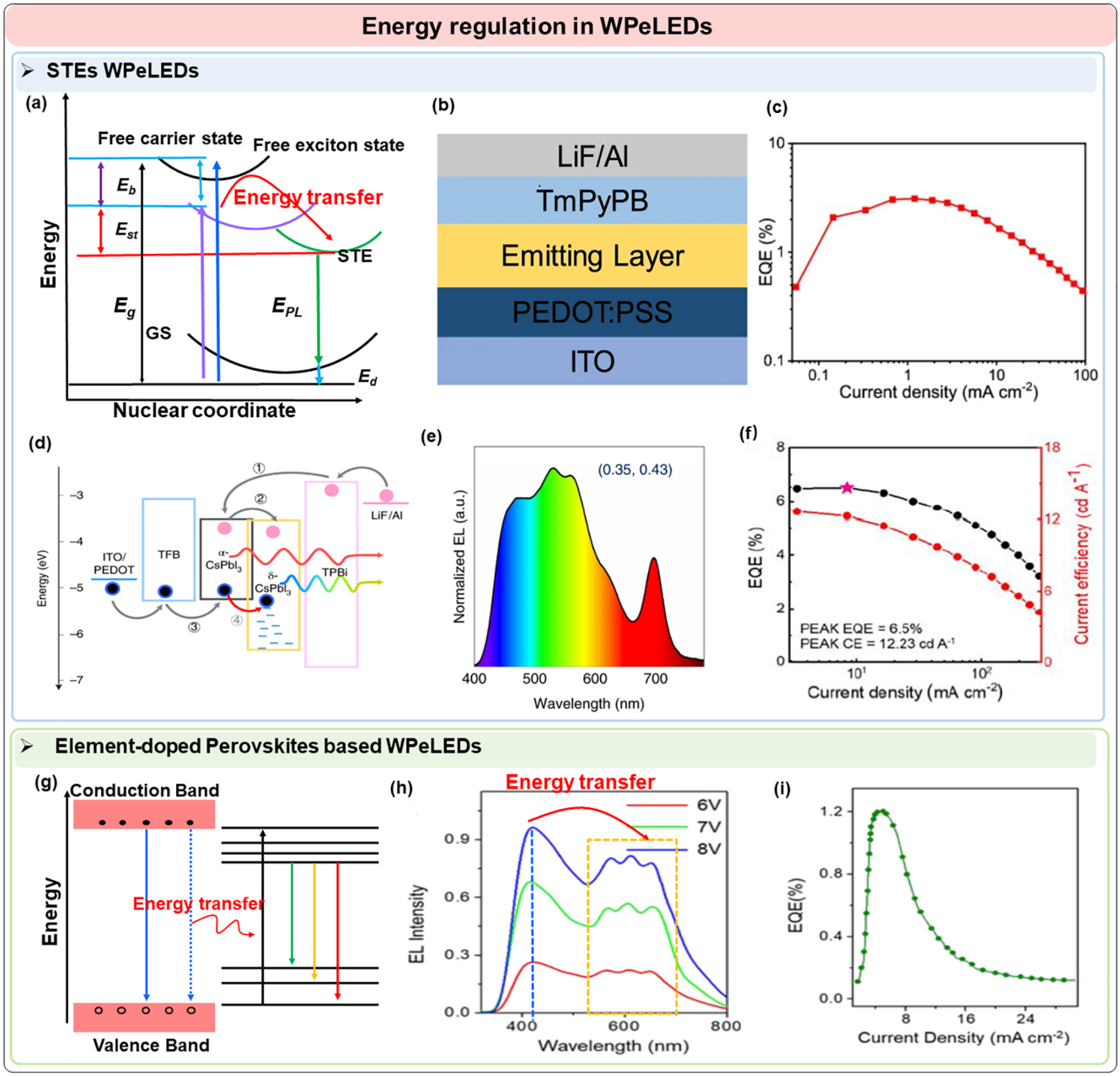


**Figure 6. Energy-transfer regulation in WPeLEDs. STE-based broadband spectrum: (a) Schematic illustration of an emissive mechanism for STEs. (b) Schematic diagram of the device structure. (c) EQE versus current density. Reprinted with permission from ref 94. Copyright 2021 Nature Publishing Group. (d) Proposed carrier injection and recombination mechanism for PeWLEDs. (e) Typical electroluminescence spectra, covering the whole visible band very well. (f) EQE and CE of the WLEDs, which exhibited efficiencies of 6.5% and 12 200 cd/m$^2$, respectively. Reprinted with permission from ref 93. Copyright 2020 Nature Publishing Group. (g) Energy-transfer mechanism of element-doped perovskite forming multi-color emissive centers. (l) Schematic of the $Sm^{3+}$ ion-doped $CsPbCl_3$ PeLED configuration. (h) EL spectra against various voltages of PeLEDs based on 5.1 mol% $Sm^{3+}$ ion-doped $CsPbCl_3$ PeNCs. (i) EQE−*J* curve of PeLEDs based on 5.1 mol% $Sm^{3+}$ ion-doped $CsPbCl_3$ PeNCs.[97]**

charge carriers from the matrix by $Sm^{3+}$, $CsPbCl_3$ NCs and $Sm^{3+}$ respectively emitted blue light and green/orange/red light at the same time, generating white light. The device exhibited an extremely stable EL spectrum (Figure 6h), benefiting from a single-component emitter with stable and efficient energy transfer. The WPeLED achieved the best EQE of 1.2% (Figure 6i) with a CRI of 93.

## SUMMARY AND OUTLOOK

In this Focus Review, we analyzed the energy-transfer mechanisms that diffusely exist in various kinds of WLEDs, including (1) carriers/excitons energy transfer between host and guest, (2) excitons cascade energy transfer among multi-color emissive centers, and (3) energy transfer in STEs. Then, we discussed approaches to regulate these energy-transfer behaviors, i.e., the selection and co-location of host and guest materials, the optimization of the doping concentrations, and


https://doi.org/10.1021/acsenergylett.2c00610
ACS Energy Lett. 2022, 7, 2173−2188

the introduction and design of interlayers or ICLs in stacked WLEDs. These approaches were widely applied in WOLEDs, WQLEDs, and WPeLEDs and enabled them to make great progress, promoting the development of lighting and display fields. Here, we summarized some research progress about WOLEDs, WQLEDs, and WPeLEDs, as shown in Table 1. In both mixed single and stacked-WOLEDs, the EQE was improved from lower than 10% at an early stage of development to over 20%.[30,40,103,104,44,63,64,98−102] Besides, by introducing complex ICLs to completely suppress energy transfer, tandem WOLEDs could achieve ultrahigh EQE.[54,67,73,105] For WQLEDs, mixed SEL- and stacked-WQLEDs cannot achieve high performance (EQE around 10%) due to energy loss in the energy-transfer process.[77,78,80−82] But using ICLs to eliminate the energy transfer among R/G/B QDs, WQLEDs can obtain EQEs higher than 20%.[83,85,106] By following energy regulation tactics used with WOLEDs and WQLEDs, emerging WPeLEDs also have successfully realized white emission on mixed SEL and stacked structures,[12,87,90,92−94,97] but the performance of WPeLEDs suffers from the restriction of perovskites' photoelectric and chemical properties, i.e., ions migration, solvent incompatibility, and poor carrier injection.

**Table 1. Summary of Representative WOLEDs, WQLEDs, and WPeLEDs**

| WLEDs | PE (lm/W) | EQE (%) | CRI | CIE (*x*, *y*) | year and ref |
|---|---|---|---|---|---|
| | | **WOLEDs** | | | |
| mixed SEL | 42.5 | 19.3 | – | (0.33, 0.39) | 2009[40] |
| | 67.2 | 26.6 | – | (0.41, 0.43) | 2015[30] |
| | 63.2 | 24 | – | (0.38, 0.48) | 2013[98] |
| | 84.1 | 25.5 | 72−76 | (0.38, 0.42) | 2015[44] |
| | 65.8 | 24.6 | 78 | (0.36, 0.47) | 2015[99] |
| | 105 | 28.1 | – | (0.48, 0.48) | 2017[100] |
| | 55.1 | 23.6 | 87 | (0.34, 0.36) | 2019[101] |
| | 94.8 | 27.5 | – | (0.45, 0.47) | 2019[102] |
| | 35.1 | 27.3 | – | (0.34, 0.40) | 2020[103] |
| stacked | 40.7 | 21.2 | – | (0.43, 0.43) | 2014[63] |
| | 36.2 | 19.7 | – | (0.35, 0.48) | 2015[104] |
| | 21.9 | 23 | – | (0.34, 0.33) | 2019[64] |
| tandem | 63 | 54.3 | – | (0.36, 0.50) | 2014[73] |
| | 33.4 | 49.4 | 93 | (0.46, 0.43) | 2018[67] |
| | 40.3 | 34.7 | 93 | (0.48, 0.43) | 2019[54] |
| | 50 | 171 | 89.4 | (0.49, 0.43) | 2018[105] |
| | | **WQLEDs** | | | |
| mixed SEL | – | 10.9 | 71−75 | – | 2015[77] |
| | – | 10.6 | – | (0.29, 0.35) | 2020[78] |
| stacked | – | 6.8 | – | (0.32, 0.33) | 2018[80] |
| | 25.8 | – | – | – | 2018[81] |
| | – | 9.6 | – | (0.34, 0.34) | 2018[82] |
| tandem | – | 23.88 | 80 | (0.33, 0.34) | 2018[83] |
| | 10.5 | 27.3 | – | (0.40, 0.38) | 2018[106] |
| | 10.92 | 28 | 75 | (0.34, 0.33) | 2018[85] |
| | | **WPeLEDs** | | | |
| mixed SEL or a single emitter | – | 0.008 | – | – | 2020[90] |
| | – | 0.08 | 94.5 | (0.32, 0.32) | 2018[91] |
| | – | – | 94 | (0.33, 0.35) | 2018[92] |
| | – | 0.15 | 91.6 | – | 2020[12] |
| | – | 3.1 | – | – | 2021[94] |
| | – | 6.5 | – | (0.35, 0.43) | 2021[93] |
| | – | 1.2 | 93 | (0.32, 0.31) | 2020[97] |
| tandem | – | – | – | (0.32, 0.32) | 2018[87] |

Considering their huge advantages and potential in energy savings, research status, and development progress, we propose some prospects for the development of WOLEDs, WQLEDs, and WPeLEDs, hoping that they can provide some inspiration for future research.

(1) WOLEDs have mature energy regulation approaches and technologies. Based on these effective strategies, the development of low-cost materials and preparation technology is a direction to strive for in the future, e.g., low-cost solution process technology.

(2) High-efficiency WQLEDs require complex structures to regulate energy, so it is a key point to design and develop new and efficient ICLs. Currently, different kinds of ICLs have been proposed and fabricated. However, WQLEDs always suffered from the limitation of these ICLs. On one hand, the compatibility of P-N is insufficient, which easily causes high interface defect density. On the other hand, the complicated processing where some films are evaporated and some are spin-coated can also affect performance.

(3) WPeLEDs have been developed by employing energy regulation methods used with WOLEDs and WQLEDs. Now, WPeLEDs are facing challenges as follows: (a) In stacked structure, there are grant technical challenges, e.g., incompatible solvents, severe interface defects, and complex preparation process. (b) In the single-EML mixed structure, suppression of ions migration is also a big challenge. Besides, in single-emitter-based WPeLEDs, especially STEs with white emission, poor carrier transport capability of STEs is the primary problem that needs to be solved. To do so, we propose, some conductive luminescent organic ligands can be introduced into perovskites,[107] which is conducive to improving the carrier transport performance and the white light quality.

(4) Light extraction technique is an effective strategy to further enhance energy utilization, especially toward light loss caused by wave-guided modes and surface plasmon polariton (SPP) modes in WLEDs.[108] Various light out-coupling techniques, such as micro-lens arrays and nanoimprint patterns, have emerged.[109−113] In the future, exploitation of convenient, high-performance, and low-cost integrated technology for WLEDs is an important direction.

(5) Considering environmental protection and the harm of heavy metals to biological systems, new luminescent materials should also be continuously exploited, especially using environment-friendly luminescent materials (e.g., InP, ZnS) as the EMLs to develop WLEDs.[114−116]

## ■ AUTHOR INFORMATION

### Corresponding Authors

**Hengyang Xiang** − *MIIT Key Laboratory of Advanced Display Materials and Devices, Institute of Optoelectronics & Nanomaterials, College of Materials Science and Engineering, Nanjing University of Science and Technology, Nanjing 210094, China*; Email: xiang.hengyang@njust.edu.cn

**Haibo Zeng** − *MIIT Key Laboratory of Advanced Display Materials and Devices, Institute of Optoelectronics & Nanomaterials, College of Materials Science and Engineering,*



https://doi.org/10.1021/acsenergylett.2c00610
ACS Energy Lett. 2022, 7, 2173−2188

*Nanjing University of Science and Technology, Nanjing 210094, China;* orcid.org/0000-0002-0281-3617; Email: zeng.haibo@njust.edu.cn

### Authors

**Run Wang** − *MIIT Key Laboratory of Advanced Display Materials and Devices, Institute of Optoelectronics & Nanomaterials, College of Materials Science and Engineering, Nanjing University of Science and Technology, Nanjing 210094, China*

**Jiawei Chen** − *MIIT Key Laboratory of Advanced Display Materials and Devices, Institute of Optoelectronics & Nanomaterials, College of Materials Science and Engineering, Nanjing University of Science and Technology, Nanjing 210094, China*

**Yan Li** − *MIIT Key Laboratory of Advanced Display Materials and Devices, Institute of Optoelectronics & Nanomaterials, College of Materials Science and Engineering, Nanjing University of Science and Technology, Nanjing 210094, China*

**Yihui Zhou** − *MIIT Key Laboratory of Advanced Display Materials and Devices, Institute of Optoelectronics & Nanomaterials, College of Materials Science and Engineering, Nanjing University of Science and Technology, Nanjing 210094, China*

**Wallace C. H. Choy** − *Department of Electrical and Electronic Engineering, The University of Hong Kong, Hong Kong 999077, China;* orcid.org/0000-0002-9535-4076

**Zhiyong Fan** − *Department of Electronic and Computer Engineering, The Hong Kong University of Science and Technology, Hong Kong 999077, China;* orcid.org/0000-0002-5397-0129

Complete contact information is available at: https://pubs.acs.org/10.1021/acsenergylett.2c00610

### Notes

The authors declare no competing financial interest.

### Biographies

**Run Wang** received her master's degree from the School of Physical Science and Technology, Southwest University, in 2020. She is now a Ph.D. student in Prof. Zeng's group. Her research interests are in light-emitting materials and optoelectronic devices.

**Hengyang Xiang** received his M.S. in Materials Science and Engineering from Soochow University in 2016 and a Ph.D. degree in Materials Physics and Chemistry from Sorbonne University in 2019. He is now a lecturer at Nanjing University of Science and Technology. His research focuses on light-emitting diodes and photodetectors based on perovskites.

**Jiawei Chen** received his bachelor's degree in Materials Physics from Nanjing University of Science and Technology in 2018. Now, he is a Ph.D. candidate in Prof. Zeng's group. His current research interests include all-inorganic halide perovskites and their optoelectronic applications.

**Yan Li** joined Prof. Zeng's group in 2020. Presently, he is studying for a master's degree at Nanjing University of Science and Technology. His research interests are in new light-emitting materials and display devices, including perovskite materials and LED devices.

**Yihui Zhou** joined Prof. Zeng's group in 2020. Currently, he is studying for a master's degree at Nanjing University of Science and Technology. His research interests are in new light-emitting materials and display devices, including perovskite materials and LED devices.

**Wallace C. H. Choy** received his Ph.D. in Electronic Engineering from the University of Surrey, UK, in 1999. He is now a professor in the Department of Electronic Engineering, The University of Hong Kong. His research interests cover organic/inorganic optoelectronic devices, plasmonic structures, metal oxides, and nanomaterial devices.

**Zhiyong Fan** received his Ph.D. in Materials Science from the University of California, Irvine, in 2006. In 2010, he joined the faculty of The Hong Kong University of Science and Technology. His interests are in the design and fabrication of nanostructures and nanomaterials, energy-harvesting devices, and sensors.

**Haibo Zeng** obtained his Ph.D. in Material Physics from the Chinese Academy of Science in 2006. He joined the faculty at Nanjing University of Science and Technology in 2011. His research interests are focused on the exploratory design of semiconducting nanocrystals and 2D crystals, with an emphasis on optoelectronics applications.

## ■ ACKNOWLEDGMENTS

This work was financially supported by the National Natural Science Foundation of China (52131304, 62004101, 61725402), the Fundamental Research Funds for the Central Universities (30919012107, 30920041117), and the China Postdoctoral Science Foundation (2020M681600).

## ■ REFERENCES

(1) Farinola, G. M.; Ragni, R. Electroluminescent Materials for White Organic Light Emitting Diodes. *Chem. Soc. Rev.* **2011**, *40* (7), 3467−3482.

(2) Reineke, S.; Thomschke, M.; Lüssem, B.; Leo, K. White Organic Light-Emitting Diodes: Status and Perspective. *Rev. Mod. Phys.* **2013**, *85* (3), 1245−1293.

(3) Chang, Y. L.; Lu, Z. H. White Organic Light-Emitting Diodes for Solid-State Lighting. *IEEE/OSA J. Dispersion Technol.* **2013**, *9* (6), 459−468.

(4) Cho, J.; Park, J. H.; Kim, J. K.; Schubert, E. F. White Light-Emitting Diodes: History, Progress, and Future. *Laser Photonics Rev.* **2017**, *11* (2), 1600147.

(5) Guner, T.; Demir, M. M. A Review on Halide Perovskites as Color Conversion Layers in White Light Emitting Diode Applications. *Phys. Status Solidi Appl. Mater. Sci.* **2018**, *215* (13), 1800120.

(6) Sheu, J.K.; Chang, S.J.; Kuo, C.H.; Su, Y.K.; Wu, L.W.; Lin, Y.C.; Lai, W.C.; Tsai, J.M.; Chi, G.C.; Wu, R.K. White-light emission from near UV InGaN-GaN LED chip precoated with blue/green/red phosphors. *IEEEPhotonics Technol. Lett.* **2003**, *15* (1), 18−20.

(7) Narukawa, Y.; Niki, I.; Izuno, K.; Yamada, M.; Murazaki, Y.; Mukai, T. Phosphor-Conversion White Light Emitting Diode Using InGaN near-Ultraviolet Chip. *Jpn. J. Appl. Phys.* **2002**, *41*, L371.

(8) Ju, H.; Wang, L.; Wang, B.; Ma, Y.; Wang, H.; Chen, S.; Tao, X. Single-Phased Emission-Tunable $Ca_3Si_2O_7$:$Ce^{3+}$, $Eu^{2+}$ Phosphors for White Light-Emitting Diodes. *Ceram. Int.* **2013**, *39* (7), 8001−8005.

(9) Wang, Z.; Li, P.; Guo, Q.; Yang, Z. A Single-Phased Warm White-Light-Emitting Phosphor $BaMg_2(PO_4)_2$:$Eu^{2+}$, $Mn^{2+}$, $Tb^{3+}$ for White Light Emitting Diodes. *Mater. Res. Bull.* **2014**, *52*, 30−36.

(10) Zhang, X.; Gong, M. Single-Phased White-Light-Emitting $NaCaBO_3$:$Ce^{3+}$, $Tb^{3+}$, $Mn^{2+}$ Phosphors for LED Applications. *Dalton Trans.* **2014**, *43* (6), 2465−2472.

(11) Huang, C. H.; Liu, W. R.; Chen, T. M. Single-Phased White-Light Phosphors $Ca_9Gd(PO_4)^7$:$Eu^{2+}$, $Mn^{2+}$ under near-Ultraviolet Excitation. *J. Phys. Chem. C* **2010**, *114* (43), 18698−18701.

(12) Ma, Z.; Shi, Z.; Yang, D.; Li, Y.; Zhang, F.; Wang, L.; Chen, X.; Wu, D.; Tian, Y.; Zhang, Y.; Zhang, L.; Li, X.; Shan, C. High Color-Rendering Index and Stable White Light-Emitting Diodes by Assembling Two Broadband Emissive Self-Trapped Excitons. *Adv. Mater.* **2021**, *33* (2), 2001367.

(13) Tsao, J. Y.; Crawford, M. H.; Coltrin, M. E.; Fischer, A. J.; Koleske, D. D.; Subramania, G. S.; Wang, G. T.; Wierer, J. J.; Karlicek,

R. F. Toward Smart and Ultra-Efficient Solid-State Lighting. *Adv. Opt. Mater.* **2014**, *2* (9), 809−836.
(14) Haitz, R.; Tsao, J. Y. Solid-State Lighting: "The Case" 10 Years after and Future Prospects. *Phys. Status Solidi Appl. Mater. Sci.* **2011**, *208* (1), 17−29.
(15) Humphreys, C. J. Solid-State Lighting. *MRS Bull.* **2008**, *33* (4), 459−470.
(16) Xiang, H.; Wang, R.; Chen, J.; Li, F.; Zeng, H. Research Progress of Full Electroluminescent White Light-Emitting Diodes Based on a Single Emissive Layer. *Light Sci. Appl.* **2021**, *10* (1), 206.
(17) Chen, J.; Xiang, H.; Wang, J.; Wang, R.; Li, Y.; Shan, Q.; Xu, X.; Dong, Y.; Wei, C.; Zeng, H. Perovskite White Light Emitting Diodes: Progress, Challenges, and Opportunities. *ACS Nano* **2021**, *15* (11), 17150−17174.
(18) Pode, R. Organic Light Emitting Diode Devices: An Energy Efficient Solid State Lighting for Applications. *Renew. Sustain. Energy Rev.* **2020**, *133*, 110043.
(19) Yuan, Q.; Wang, T.; Yu, P.; Zhang, H.; Zhang, H.; Ji, W. A Review on the Electroluminescence Properties of Quantum-Dot Light-Emitting Diodes. *Org. Electron.* **2021**, *90*, 106086.
(20) Moon, H.; Lee, C.; Lee, W.; Kim, J.; Chae, H. Stability of Quantum Dots, Quantum Dot Films, and Quantum Dot Light-Emitting Diodes for Display Applications. *Adv. Mater.* **2019**, *31* (34), 1804294.
(21) Xu, L.; Yuan, S.; Zeng, H.; Song, J. A Comprehensive Review of Doping in Perovskite Nanocrystals/Quantum Dots: Evolution of Structure, Electronics, Optics, and Light-Emitting Diodes. *Mater. Today Nano* **2019**, *6*, 100036.
(22) Yang, Z.; Gao, M.; Wu, W.; Yang, X.; Sun, X. W.; Zhang, J.; Wang, H. C.; Liu, R. S.; Han, C. Y.; Yang, H.; Li, W. Recent Advances in Quantum Dot-Based Light-Emitting Devices: Challenges and Possible Solutions. *Mater. Today* **2019**, *24*, 69−93.
(23) Quan, L. N.; García de Arquer, F. P.; Sabatini, R. P.; Sargent, E. H. Perovskites for Light Emission. *Adv. Mater.* **2018**, *30* (45), 1801996.
(24) Gather, M. C.; Köhnen, A.; Meerholz, K. White Organic Light-Emitting Diodes. *Adv. Mater.* **2011**, *23* (2), 233−248.
(25) Xiao, L.; Chen, Z.; Qu, B.; Luo, J.; Kong, S.; Gong, Q.; Kido, J. Recent Progresses on Materials for Electrophosphorescent Organic Light-Emitting Devices. *Adv. Mater.* **2011**, *23* (8), 926−952.
(26) Kamtekar, K. T.; Monkman, A. P.; Bryce, M. R. Recent Advances in White Organic Light-Emitting Materials and Devices (WOLEDS). *Adv. Mater.* **2010**, *22* (5), 572−582.
(27) Wood, V.; Bulović, V. Colloidal Quantum Dot Light-Emitting Devices. *Nano Rev.* **2010**, *1* (1), 5202.
(28) Ye, S.; Xiao, F.; Pan, Y. X.; Ma, Y. Y.; Zhang, Q. Y. Phosphors in Phosphor-Converted White Light-Emitting Diodes: Recent Advances in Materials, Techniques and Properties. *Mater. Sci. Eng. R Reports* **2010**, *71* (1), 1−34.
(29) Dai, Q.; Duty, C. E.; Hu, M. Z. Semiconductor-Nanocrystals-Based White Light-Emitting Diodes. *Small* **2010**, *6* (15), 1577−1588.
(30) Ye, J.; Zheng, C. J.; Ou, X. M.; Zhang, X. H.; Fung, M. K.; Lee, C. S. Management of Singlet and Triplet Excitons in a Single Emission Layer: A Simple Approach for a High-Efficiency Fluorescence/Phosphorescence Hybrid White Organic Light-Emitting Device. *Adv. Mater.* **2012**, *24* (25), 3410−3414.
(31) Sasaki, S.; Drummen, G. P. C.; Konishi, G. I. Recent Advances in Twisted Intramolecular Charge Transfer (TICT) Fluorescence and Related Phenomena in Materials Chemistry. *J. Mater. Chem. C* **2016**, *4* (14), 2731−2743.
(32) Ansari, M. I. H.; Qurashi, A.; Nazeeruddin, M. K. Frontiers, Opportunities, and Challenges in Perovskite Solar Cells: A Critical Review. *J. Photochem. Photobiol. C Photochem. Rev.* **2018**, *35*, 1−24.
(33) Koh, T. M.; Thirumal, K.; Soo, H. S.; Mathews, N. Multidimensional Perovskites: A Mixed Cation Approach Towards Ambient Stable and Tunable Perovskite Photovoltaics. *ChemSusChem* **2016**, *9* (18), 2541−2558.
(34) Koh, T. M.; Shanmugam, V.; Schlipf, J.; Oesinghaus, L.; Müller-Buschbaum, P.; Ramakrishnan, N.; Swamy, V.; Mathews, N.; Boix, P. P.; Mhaisalkar, S. G. Nanostructuring Mixed-Dimensional Perovskites: A Route Toward Tunable, Efficient Photovoltaics. *Adv. Mater.* **2016**, *28* (19), 3653−3661.
(35) Liu, B.; Wang, L.; Gao, D.; Xu, M.; Zhu, X.; Zou, J.; Lan, L.; Ning, H.; Peng, J.; Cao, Y. Harnessing Charge and Exciton Distribution towards Extremely High Performance: The Critical Role of Guests in Single-Emitting-Layer White OLEDs. *Mater. Horizons* **2015**, *2* (5), 536−544.
(36) Wang, Q.; Zhang, Y. X.; Yuan, Y.; Hu, Y.; Tian, Q. S.; Jiang, Z. Q.; Liao, L. S. Alleviating Efficiency Roll-Off of Hybrid Single-Emitting Layer WOLED Utilizing Bipolar TADF Material as Host and Emitter. *ACS Appl. Mater. Interfaces* **2019**, *11* (2), 2197−2204.
(37) Zhang, D.; Cai, M.; Zhang, Y.; Zhang, D.; Duan, L. Highly Efficient Simplified Single-Emitting-Layer Hybrid WOLEDs with Low Roll-off and Good Color Stability through Enhanced Förster Energy Transfer. *ACS Appl. Mater. Interfaces* **2015**, *7* (51), 28693−28700.
(38) Zou, S. J.; Zeng, X. Y.; Li, Y. Q.; Tang, J. X. The Strategies for High-Performance Single-Emissive-Layer White Organic Light-Emitting Diodes. *Laser Photonics Rev.* **2021**, *15* (3), 2000474.
(39) Kido, J.; Hongawa, K.; Okuyama, K.; Nagai, K. White Light-Emitting Organic Electroluminescent Devices Using the Poly(N-Vinylcarbazole) Emitter Layer Doped with Three Fluorescent Dyes. *Appl. Phys. Lett.* **1994**, *64* (7), 815−817.
(40) Wang, B. Q.; Ding, J.; Ma, D.; Cheng, Y.; Wang, L.; Jing, X.; Wang, F. Harvesting Excitons Via Two Parallel Channels for Efficient White Organic LEDs with Nearly 100% Internal Quantum Efficiency : Fabrication and Emission- Mechanism Analysis. *Adv. Funct. Mater.* **2009**, *19*, 84−95.
(41) Hou, L.; Duan, L.; Qiao, J.; Zhang, D.; Dong, G.; Wang, L.; Qiu, Y. Efficient Solution-Processed Small-Molecule Single Emitting Layer Electrophosphorescent White Light-Emitting Diodes. *Org. Electron.* **2010**, *11* (8), 1344−1350.
(42) Zhang, M.; Zheng, C.-J.; Wang, K.; Shi, Y.-Z.; Yang, H.-Y.; Lin, H.; Tao, S.-L.; Zhang, X.-H. Efficient and Stable Single-Emitting-Layer White Organic Light-Emitting Diodes by Employing All Thermally Activated Delayed Fluorescence Emitters. *Org. Electron.* **2022**, *101*, 106415.
(43) Chen, J.; Zhao, F.; Ma, D. Hybrid White OLEDs with Fluorophors and Phosphors. *Mater. Today* **2014**, *17* (4), 175−183.
(44) Liu, X.-K.; Chen, Z.; Qing, J.; Zhang, W.-J.; Wu, B.; Tam, H. L.; Zhu, F.; Zhang, X.-H.; Lee, C.-S. Remanagement of Singlet and Triplet Excitons in Single-Emissive-Layer Hybrid White Organic Light-Emitting Devices Using Thermally Activated Delayed Fluorescent Blue Exciplex. *Adv. Mater.* **2015**, *27* (44), 7079−7085.
(45) Zhao, F.; Wei, Y.; Xu, H.; Chen, D.; Ahamad, T.; Alshehri, S.; Pei, Q.; Ma, D. Spatial Exciton Allocation Strategy with Reduced Energy Loss for High-Efficiency Fluorescent/Phosphorescent Hybrid White Organic Light-Emitting Diodes. *Mater. Horizons* **2017**, *4* (4), 641−648.
(46) D'Andrade, B. B. W.; Holmes, R. J.; Forrest, S. R. Efficient Organic Electrophosphorescent White-Light-Emitting Device with a Triple Doped Emissive Layer. *Adv. Mater.* **2004**, *16* (7), 624−628.
(47) Schwartz, G.; Reineke, S.; Rosenow, T. C.; Walzer, K.; Leo, K. Triplet Harvesting in Hybrid White Organic Light-Emitting Diodes. *Adv. Funct. Mater.* **2009**, *19* (9), 1319−1333.
(48) Gupta, D.; Katiyar, M.; Deepak. Various Approaches to White Organic Light Emitting Diodes and Their Recent Advancements. *Opt. Mater.* **2006**, *28* (4), 295−301.
(49) Sun, N.; Wang, Q.; Zhao, Y.; Chen, Y.; Yang, D.; Zhao, F.; Chen, J.; Ma, D. High-Performance Hybrid White Organic Light-Emitting Devices without Interlayer between Fluorescent and Phosphorescent Emissive Regions. *Adv. Mater.* **2014**, *26* (10), 1617−1621.
(50) Zhu, L.; Wu, Z.; Chen, J.; Ma, D. Reduced Efficiency Roll-off in All-Phosphorescent White Organic Light-Emitting Diodes with an External Quantum Efficiency of over 20%. *J. Mater. Chem. C* **2015**, *3* (14), 3304−3310.
(51) Wu, Z.; Luo, J.; Sun, N.; Zhu, L.; Sun, H.; Yu, L.; Yang, D.; Qiao, X.; Chen, J.; Yang, C.; Ma, D. High-Performance Hybrid White Organic Light-Emitting Diodes with Superior Efficiency/Color Rendering Index/Color Stability and Low Efficiency Roll-Off Based on a Blue

Thermally Activated Delayed Fluorescent Emitter. *Adv. Funct. Mater.* **2016**, *26* (19), 3306−3313.
(52) Ying, S.; Sun, Q.; Dai, Y.; Yang, D.; Qiao, X.; Ma, D. Precise Regulation of the Emissive Layer for Ultra-High Performance White Organic Light-Emitting Diodes in an Exciplex Forming Co-Host System. *Mater. Chem. Front.* **2019**, *3* (4), 640−649.
(53) Reineke, S.; Lindner, F.; Schwartz, G.; Seidler, N.; Walzer, K.; Lüssem, B.; Leo, K. White Organic Light-Emitting Diodes with Fluorescent Tube Efficiency. *Nature* **2009**, *459* (7244), 234−238.
(54) Miao, Y.; Wei, X.; Gao, L.; Wang, K.; Zhao, B.; Wang, Z.; Zhao, B.; Wang, H.; Wu, Y.; Xu, B. Tandem White Organic Light-Emitting Diodes Stacked with Two Symmetrical Emitting Units Simultaneously Achieving Superior Efficiency/CRI/Color Stability. *Nanophotonics* **2019**, *8* (10), 1783−1794.
(55) Higuchi, T.; Nakanotani, H.; Adachi, C. High-Efficiency White Organic Light-Emitting Diodes Based on a Blue Thermally Activated Delayed Fluorescent Emitter Combined with Green and Red Fluorescent Emitters. *Adv. Mater.* **2015**, *27* (12), 2019−2023.
(56) Li, X. L.; Xie, G.; Liu, M.; Chen, D.; Cai, X.; Peng, J.; Cao, Y.; Su, S. J. High-Efficiency WOLEDs with High Color-Rendering Index Based on a Chromaticity-Adjustable Yellow Thermally Activated Delayed Fluorescence Emitter. *Adv. Mater.* **2016**, *28* (23), 4614−4619.
(57) Liu, B.; Wang, L.; Xu, M.; Tao, H.; Zou, J.; Gao, D.; Lan, L.; Ning, H.; Peng, J.; Cao, Y. Efficient Hybrid White Organic Light-Emitting Diodes with Extremely Long Lifetime: The Effect of n-Type Interlayer. *Sci. Rep.* **2015**, *4*, 7198.
(58) Ho, C. L.; Lin, M. F.; Wong, W. Y.; Wong, W. K.; Chen, C. H. High-Efficiency and Color-Stable White Organic Light-Emitting Devices Based on Sky Blue Electrofluorescence and Orange Electrophosphorescence. *Appl. Phys. Lett.* **2008**, *92* (8), 083301.
(59) Luo, D.; Yang, Y.; Xiao, Y.; Zhao, Y.; Yang, Y.; Liu, B. Regulating Charge and Exciton Distribution in High-Performance Hybrid White Organic Light-Emitting Diodes with n-Type Interlayer Switch. *Nano-Micro Lett.* **2017**, *9* (4), 1−8.
(60) Ho, C. L.; Wong, W. Y.; Wang, Q.; Ma, D.; Wang, L.; Lin, Z. A Multifunctional Iridium-Carbazolyl Orange Phosphor for High-Performance Two-Element WOLED Exploiting Exciton-Managed Fluorescence/Phosphorescence. *Adv. Funct. Mater.* **2008**, *18* (6), 928−937.
(61) Zhang, L. J.; Hua, Y. L.; Wu, X. M.; Wang, Y.; Yin, S. G. White Organic Light-Emitting Device with Both Phosphorescent and Fluorescent Emissive Layers. *Chinese Phys. B* **2008**, *17* (8), 3097−3102.
(62) Sun, Y.; Giebink, N. C.; Kanno, H.; Ma, B.; Thompson, M. E.; Forrest, S. R. Management of Singlet and Triplet Excitons for Efficient White Organic Light-Emitting Devices. *Nature* **2006**, *440* (7086), 908−912.
(63) Sun, N.; Wang, Q.; Zhao, Y.; Yang, D.; Zhao, F.; Chen, J.; Ma, D. A Hybrid White Organic Light-Emitting Diode with above 20% External Quantum Efficiency and Extremely Low Efficiency Roll-Off. *J. Mater. Chem. C* **2014**, *2* (36), 7494−7504.
(64) Chen, X.; Yang, Z.; Li, W.; Mao, Z.; Zhao, J.; Zhang, Y.; Wu, Y. C.; Jiao, S.; Liu, Y.; Chi, Z. Nondoped Red Fluorophores with Hybridized Local and Charge-Transfer State for High-Performance Fluorescent White Organic Light-Emitting Diodes. *ACS Appl. Mater. Interfaces* **2019**, *11* (42), 39026−39034.
(65) Zhang, S.; Yue, S.; Wu, Q.; Zhang, Z.; Chen, Y.; Wang, X.; Liu, Z.; Xie, G.; Xue, Q.; Qu, D.; Zhao, Y.; Liu, S. Color Stable Multilayer All-Phosphor White Organic Light-Emitting Diodes with Excellent Color Quality. *Org. Electron.* **2013**, *14* (8), 2014−2022.
(66) Son, Y. H.; Park, M. J.; Kim, Y. J.; Yang, J. H.; Park, J. S.; Kwon, J. H. Color Stable Phosphorescent White Organic Light-Emitting Diodes with Double Emissive Layer Structure. *Org. Electron.* **2013**, *14* (4), 1183−1188.
(67) Park, M. J.; Son, Y. H.; Yang, H. I.; Kim, S. K.; Lampande, R.; Kwon, J. H. Optical Design and Optimization of Highly Efficient Sunlight-like Three-Stacked Warm White Organic Light Emitting Diodes. *ACS Photonics* **2018**, *5* (2), 655−662.
(68) Fung, M. K.; Li, Y. Q.; Liao, L. S. Tandem Organic Light-Emitting Diodes. *Adv. Mater.* **2016**, *28* (47), 10381−10408.
(69) Wang, J.; Wang, Y.; Qin, Y.; Li, R.; An, J.; Chen, Y.; Lai, W.-Y.; Zhang, X.; Huang, W. Highly Efficient Ultra-Flexible Tandem Organic Light-Emitting Diodes Adopting a Non-Doped Charge Generation Unit. *J. Mater. Chem. C* **2021**, *9* (27), 8570−8578.
(70) Shi, C.; Sun, N.; Wu, Z.; Chen, J.; Ma, D. High Performance Hybrid Tandem White Organic Light-Emitting Diodes by Using a Novel Intermediate Connector. *J. Mater. Chem. C* **2018**, *6* (4), 767−772.
(71) Cho, H.; Song, J.; Kwon, B.-H.; Choi, S.; Lee, H.; Joo, C. W.; Ahn, S.-D.; Kang, S.-Y.; Yoo, S.; Moon, J. Stabilizing Color Shift of Tandem White Organic Light-Emitting Diodes. *J. Ind. Eng. Chem.* **2019**, *69*, 414−421.
(72) Liu, B.; Wang, L.; Tao, H.; Xu, M.; Zou, J.; Ning, H.; Peng, J.; Cao, Y. Doping-Free Tandem White Organic Light-Emitting Diodes. *Sci. Bull.* **2017**, *62* (17), 1193−1200.
(73) Lee, S.; Shin, H.; Kim, J.-J. High-Efficiency Orange and Tandem White Organic Light-Emitting Diodes Using Phosphorescent Dyes with Horizontally Oriented Emitting Dipoles. *Adv. Mater.* **2014**, *26* (33), 5864−5868.
(74) Guo, F.; Ma, D. White Organic Light-Emitting Diodes Based on Tandem Structures. *Appl. Phys. Lett.* **2005**, *87* (17), 173510.
(75) Kanno, H.; Holmes, R. J.; Sun, Y.; Kena-Cohen, S.; Forrest, S. R. White Stacked Electrophosphorescent Organic Light-Emitting Devices Employing MoO3 as a Charge-Generation Layer. *Adv. Mater.* **2006**, *18* (3), 339−342.
(76) Anikeeva, P. O.; Halpert, J. E.; Bawendi, M. G.; Bulović, V. Electroluminescence from a Mixed Red-Green-Blue Colloidal Quantum Dot Monolayer. *Nano Lett.* **2007**, *7* (8), 2196−2200.
(77) Lee, K.-H.; Han, C.-Y.; Kang, H.-D.; Ko, H.; Lee, C.; Lee, J.; Myoung, N.; Yim, S.-Y.; Yang, H. Highly Efficient, Color-Reproducible Full-Color Electroluminescent Devices Based on Red/Green/Blue Quantum Dot-Mixed Multilayer. *ACS Nano* **2015**, *9* (11), 10941−10949.
(78) Zhu, Y.; Xu, R.; Zhou, Y.; Xu, Z.; Liu, Y.; Tian, F.; Zheng, X.; Ma, F.; Alsharafi, R.; Hu, H.; Guo, T.; Kim, T. W.; Li, F. Ultrahighly Efficient White Quantum Dot Light-Emitting Diodes Operating at Low Voltage. *Adv. Opt. Mater.* **2020**, *8* (24), 2001479.
(79) Kim, T. H.; Chung, D. Y.; Ku, J.; Song, I.; Sul, S.; Kim, D. H.; Cho, K. S.; Choi, B. L.; Min Kim, J.; Hwang, S.; Kim, K. Heterogeneous Stacking of Nanodot Monolayers by Dry Pick-and-Place Transfer and Its Applications in Quantum Dot Light-Emitting Diodes. *Nat. Commun.* **2013**, *4* (1), 1−12.
(80) Lee, K. H.; Han, C. Y.; Jang, E. P.; Jo, J. H.; Hong, S.; Hwang, J. Y.; Choi, E.; Hwang, J. H.; Yang, H. Full-Color Capable Light-Emitting Diodes Based on Solution-Processed Quantum Dot Layer Stacking. *Nanoscale* **2018**, *10* (14), 6300−6305.
(81) Wang, L.; Pan, J.; Qian, J.; Lei, W.; Wu, Y.; Zhang, W.; Goto, D. K.; Chen, J. A Highly Efficient White Quantum Dot Light-Emitting Diode Employing Magnesium Doped Zinc Oxide as the Electron Transport Layer Based on Bilayered Quantum Dot Layers. *J. Mater. Chem. C* **2018**, *6* (30), 8099−8104.
(82) Chang, C.; Zhang, Q.; Zhao, W.; Li, F.; Huang, Y.; Li, L.; Shen, H.; Li, Q. Highly Efficient Trilayered White Quantum Dot Light Emitting Diodes Based on Organic Buffer Layers. *IEEE Electron Device Lett.* **2018**, *39* (11), 1692−1695.
(83) Zhang, H.; Su, Q.; Sun, Y.; Chen, S. Efficient and Color Stable White Quantum-Dot Light-Emitting Diodes with External Quantum Efficiency Over 23%. *Adv. Opt. Mater.* **2018**, *6* (16), 1800354.
(84) Jiang, C.; Zou, J.; Liu, Y.; Song, C.; He, Z.; Zhong, Z.; Wang, J.; Yip, H.-L.; Peng, J.; Cao, Y. Fully Solution-Processed Tandem White Quantum-Dot Light-Emitting Diode with an External Quantum Efficiency Exceeding 25%. *ACS Nano* **2018**, *12* (6), 6040−6049.
(85) Cao, F.; Zhao, D.; Shen, P.; Wu, J.; Wang, H.; Wu, Q.; Wang, F.; Yang, X. High-Efficiency, Solution-Processed White Quantum Dot Light-Emitting Diodes with Serially Stacked Red/Green/Blue Units. *Adv. Opt. Mater.* **2018**, *6* (20), 1800652.
(86) Yu, H.; Wang, H.; Pozina, G.; Yin, C.; Liu, X. K.; Gao, F. Single-Emissive-Layer All-Perovskite White Light-Emitting Diodes Employing

Segregated Mixed Halide Perovskite Crystals. *Chem. Sci.* **2020**, *11* (41), 11338−11343.

(87) Mao, J.; Lin, H.; Ye, F.; Qin, M.; Burkhartsmeyer, J. M.; Zhang, H.; Lu, X.; Wong, K. S.; Choy, W. C. H. All-Perovskite Emission Architecture for White Light-Emitting Diodes. *ACS Nano* **2018**, *12*, 10486−10492.

(88) Liu, D.; Liu, X.; Gan, Y.; Liu, Z.; Sun, G.; Shen, C.; Peng, X.; Qiu, W.; Li, D.; Zhou, Z.; Li, Z.; Yip, H. L.; Su, S. J. Perovskite/Organic Hybrid White Electroluminescent Devices with Stable Spectrum and Extended Operating Lifetime. *ACS Energy Lett.* **2022**, *7* (1), 523−532.

(89) Li, S.; Luo, J.; Liu, J.; Tang, J. Self-Trapped Excitons in All-Inorganic Halide Perovskites: Fundamentals, Status, and Potential Applications. *J. Phys. Chem. Lett.* **2019**, *10* (8), 1999−2007.

(90) Luo, J.; Wang, X.; Li, S.; Liu, J.; Guo, Y.; Niu, G.; Yao, L.; Fu, Y.; Gao, L.; Dong, Q.; Zhao, C.; Leng, M.; Ma, F.; Liang, W.; Wang, L.; Jin, S.; Han, J.; Zhang, L.; Etheridge, J.; Wang, J.; Yan, Y.; Sargent, E. H.; Tang, J. Efficient and Stable Emission of Warm-White Light from Lead-Free Halide Double Perovskites. *Nature* **2018**, *563* (7732), 541−545.

(91) Zhang, Y.; Zhang, Z.; Yu, W.; He, Y.; Chen, Z.; Xiao, L.; Shi, J. J.; Guo, X.; Wang, S.; Qu, B. Lead-Free Double Perovskite Cs2AgIn0.9-Bi0.1Cl6 Quantum Dots for White Light-Emitting Diodes. *Adv. Sci.* **2022**, *9* (2), 2102895.

(92) Liu, S.; Yue, Y.; Zhang, X.; Wang, C.; Yang, G.; Zhu, D. A Controllable and Reversible Phase Transformation between All-Inorganic Perovskites for White Light Emitting Diodes. *J. Mater. Chem. C* **2020**, *8* (25), 8374−8379.

(93) Chen, J.; Wang, J.; Xu, X.; Li, J.; Song, J.; Lan, S.; Liu, S.; Cai, B.; Han, B.; Precht, J. T.; Ginger, D.; Zeng, H. Efficient and Bright White Light-Emitting Diodes Based on Single-Layer Heterophase Halide Perovskites. *Nat. Photonics* **2021**, *15* (3), 238−244.

(94) Chen, H.; Zhu, L.; Xue, C.; Liu, P.; Du, X.; Wen, K.; Zhang, H.; Xu, L.; Xiang, C.; Lin, C.; Qin, M.; Zhang, J.; Jiang, T.; Yi, C.; Cheng, L.; Zhang, C.; Yang, P.; Niu, M.; Xu, W.; Lai, J.; Cao, Y.; Chang, J.; Tian, H.; Jin, Y.; Lu, X.; Jiang, L.; Wang, N.; Huang, W.; Wang, J. Efficient and Bright Warm-White Electroluminescence from Lead-Free Metal Halides. *Nat. Commun.* **2021**, *12*, 1421.

(95) Liu, W.; Lin, Q.; Li, H.; Wu, K.; Robel, I.; Pietryga, J. M.; Klimov, V. I. Mn2+-Doped Lead Halide Perovskite Nanocrystals with Dual-Color Emission Controlled by Halide Content. *J. Am. Chem. Soc.* **2016**, *138* (45), 14954−14961.

(96) Huang, G.; Wang, C.; Xu, S.; Zong, S.; Lu, J.; Wang, Z.; Lu, C.; Cui, Y. Postsynthetic Doping of MnCl2Molecules into Preformed CsPbBr3 Perovskite Nanocrystals via a Halide Exchange-Driven Cation Exchange. *Adv. Mater.* **2017**, *29* (29), 1700095.

(97) Sun, R.; Lu, P.; Zhou, D.; Xu, W.; Ding, N.; Shao, H.; Zhang, Y.; Li, D.; Wang, N.; Zhuang, X.; Dong, B.; Bai, X.; Song, H. Samarium-Doped Metal Halide Perovskite Nanocrystals for Single-Component Electroluminescent White Light-Emitting Diodes. *ACS Energy Lett.* **2020**, *5* (7), 2131−2139.

(98) Dong, S.-C.; Liu, Y.; Li, Q.; Cui, L.-S.; Chen, H.; Jiang, Z.-Q.; Liao, L.-S. Spiro-Annulated Triarylamine-Based Hosts Incorporating Dibenzothiophene for Highly Efficient Single-Emitting Layer White Phosphorescent Organic Light-Emitting Diodes. *J. Mater. Chem. C* **2013**, *1* (40), 6575−6584.

(99) Xie, Y.-M.; Cui, L.-S.; Liu, Y.; Zu, F.-S.; Li, Q.; Jiang, Z.-Q.; Liao, L.-S. Efficient Blue/White Phosphorescent Organic Light-Emitting Diodes Based on a Silicon-Based Host Material via a Direct Carbon-Nitrogen Bond. *J. Mater. Chem. C* **2015**, *3* (20), 5347−5353.

(100) Wu, S. F.; Li, S. H.; Wang, Y. K.; Huang, C. C.; Sun, Q.; Liang, J. J.; Liao, L. S.; Fung, M. K. White Organic LED with a Luminous Efficacy Exceeding 100 Lm W-1 without Light Out-Coupling Enhancement Techniques. *Adv. Funct. Mater.* **2017**, *27* (31), 1701314.

(101) Tanaka, M.; Noda, H.; Nakanotani, H.; Adachi, C. Effect of Carrier Balance on Device Degradation of Organic Light-Emitting Diodes Based on Thermally Activated Delayed Fluorescence Emitters. *Adv. Electron. Mater.* **2019**, *5* (5), 1800708.

(102) Cao, C.; Chen, W. C.; Chen, J. X.; Yang, L.; Wang, X. Z.; Yang, H.; Huang, B.; Zhu, Z. L.; Tong, Q. X.; Lee, C. S. Bipolar Blue Host Emitter with Unity Quantum Yield Allows Full Exciton Radiation in Single-Emissive-Layer Hybrid White Organic Light-Emitting Diodes. *ACS Appl. Mater. Interfaces* **2019**, *11* (12), 11691−11698.

(103) Xie, F.-M.; An, Z.-D.; Xie, M.; Li, Y.-Q.; Zhang, G.-H.; Zou, S.-J.; Chen, L.; Chen, J.-D.; Cheng, T.; Tang, J.-X. Tert-Butyl Substituted Hetero-Donor TADF Compounds for Efficient Solution-Processed Non-Doped Blue OLEDs. *J. Mater. Chem. C* **2020**, *8* (17), 5769−5776.

(104) Li, X. L.; Ouyang, X.; Liu, M.; Ge, Z.; Peng, J.; Cao, Y.; Su, S. J. Highly Efficient Single- and Multi-Emission-Layer Fluorescent/Phosphorescent Hybrid White Organic Light-Emitting Diodes with ∼ 20% External Quantum Efficiency. *J. Mater. Chem. C* **2015**, *3* (35), 9233−9239.

(105) Coburn, C.; Jeong, C.; Forrest, S. R. Reliable, All-Phosphorescent Stacked White Organic Light Emitting Devices with a High Color Rendering Index. *ACS Photonics* **2018**, *5* (2), 630−635.

(106) Jiang, C.; Zou, J.; Liu, Y.; Song, C.; He, Z.; Zhong, Z.; Wang, J.; Yip, H. L.; Peng, J.; Cao, Y. Fully Solution-Processed Tandem White Quantum-Dot Light-Emitting Diode with an External Quantum Efficiency Exceeding 25%. *ACS Nano* **2018**, *12* (6), 6040−6049.

(107) Huang, Q.; Yang, S.; Feng, S.; Zhen, H.; Lin, Z.; Ling, Q. Multicolor Output from 2D Hybrid Perovskites with Wide Band Gap: Highly Efficient White Emission, Dual-Color Afterglow, and Switch between Fluorescence and Phosphorescence. *J. Phys. Chem. Lett.* **2021**, *12* (3), 1040−1045.

(108) Saxena, K.; Jain, V. K.; Mehta, D. S. A Review on the Light Extraction Techniques in Organic Electroluminescent Devices. *Opt. Mater.* **2009**, *32* (1), 221−233.

(109) Wang, S.; Dou, X.; Chen, L.; Fang, Y.; Wang, A.; Shen, H.; Du, Z. Enhanced Light Out-Coupling Efficiency of Quantum Dot Light Emitting Diodes by Nanoimprint Lithography. *Nanoscale* **2018**, *10* (24), 11651−11656.

(110) Zhang, Q.; Tavakoli, M. M.; Gu, L.; Zhang, D.; Tang, L.; Gao, Y.; Guo, J.; Lin, Y.; Leung, S.-F.; Poddar, S.; Fu, Y.; Fan, Z. Efficient Metal Halide Perovskite Light-Emitting Diodes with Significantly Improved Light Extraction on Nanophotonic Substrates. *Nat. Commun.* **2019**, *10* (1), 727.

(111) Ding, K.; Fang, Y.; Dong, S.; Chen, H.; Luo, B.; Jiang, K.; Gu, H.; Fan, L.; Liu, S.; Hu, B.; Wang, L. 24.1% External Quantum Efficiency of Flexible Quantum Dot Light-Emitting Diodes by Light Extraction of Silver Nanowire Transparent Electrodes. *Adv. Opt. Mater.* **2018**, *6* (19), 1800347.

(112) Xiang, H. Y.; Li, Y. Q.; Meng, S. S.; Lee, C. S.; Chen, L. S.; Tang, J. X. Extremely Efficient Transparent Flexible Organic Light-Emitting Diodes with Nanostructured Composite Electrodes. *Adv. Opt. Mater.* **2018**, *6* (21), 1800831.

(113) Xiang, H. Y.; Li, Y. Q.; Zhou, L.; Xie, H. J.; Li, C.; Ou, Q. D.; Chen, L. S.; Lee, C. S.; Lee, S. T.; Tang, J. X. Outcoupling-Enhanced Flexible Organic Light-Emitting Diodes on Ameliorated Plastic Substrate with Built-in Indium-Tin-Oxide-Free Transparent Electrode. *ACS Nano* **2015**, *9* (7), 7553−7562.

(114) Zhang, Y.; Xie, C.; Su, H.; Liu, J.; Pickering, S.; Wang, Y.; Yu, W. W.; Wang, J.; Wang, Y.; Hahm, J. I.; Dellas, N.; Mohney, S. E.; Xu, J. Employing Heavy Metal-Free Colloidal Quantum Dots in Solution-Processed White Light-Emitting Diodes. *Nano Lett.* **2011**, *11* (2), 329−332.

(115) Yang, X.; Zhao, D.; Leck, K. S.; Tan, S. T.; Tang, Y. X.; Zhao, J.; Demir, H. V.; Sun, X. W. Full Visible Range Covering InP/ZnS Nanocrystals with High Photometric Performance and Their Application to White Quantum Dot Light-Emitting Diodes. *Adv. Mater.* **2012**, *24* (30), 4180−4185.

(116) Yang, X.; Divayana, Y.; Zhao, D.; Swee Leck, K.; Lu, F.; Tiam Tan, S.; Putu Abiyasa, A.; Zhao, Y.; Volkan Demir, H.; Wei Sun, X. A Bright Cadmium-Free, Hybrid Organic/Quantum Dot White Light-Emitting Diode. *Appl. Phys. Lett.* **2012**, *101* (23), 233110.